According to the magnetic anomaly map, the prominent anomalies are the E-W trending magnetic lineation formed by the seafloor spreading and the reversal of geomagnetism, N-S trending magnetic lineation caused by transform fault and a positive/negative anomaly pair associated with the seamounts.

3) Three-Dimensional Inversion Solution

In the first stage of analysis, to express a positive/negative pair anomaly as a single anomaly, we created "reduction to the pole anomaly derived from total magnetic anomaly". We adopted reduction to the pole anomaly map assumed the inclination 28° S (Figure 3-2-3-1), which was the optimum one compared with several inclination map.

The analysis of magnetization was made on the assumption that a three-dimensional magnetic source model was divided by 2 x 2 km prisms with an upper surface defined by bathymetry and flat bottom. The depth to the bottom discovered by the power spectrum were the 14.0 km, which (depth) was interpreted as the Curie isotherm.

Then, we calculate the sum of the magnetic force due to prisms within the calculative region of 100 x 100 km. And each prism's intensity of magnetization was increased or decreased by matching the value of these calculated anomaly and the reduction to the pole anomaly.

We iterated this procedure until matching the value of calculated and the reduction to the pole anomaly. Then, a magnetization distribution map (Figure 3-2-3-2) was created by fixing the intensity of magnetization of every prism.

4) The Outline of the Magnetization Distribution Map

(1) Magnetic Lineation

Magnetic anomalies will reveal as lineation caused by the seafloor spreading and by the reversal of geomagnetism.

The major magnetic anomalies are numbered as follows;

Anomaly 1 : ～0.72 Ma (Brunhes Normal Epoch)
Anomaly J : 0.91-0.97 Ma (Jaramillo Normal Event within Matuyama Reversed Epoch)
Anomaly 2 : 1.66-1.87 Ma (Within Matuyama Reversed Epoch)
Anomaly 2': 2.47-3.40 Ma (Within Matuyama Reversed Epoch)
Anomaly 3 : 3.86-4.79 Ma (Within Matuyama Reversed Epoch)

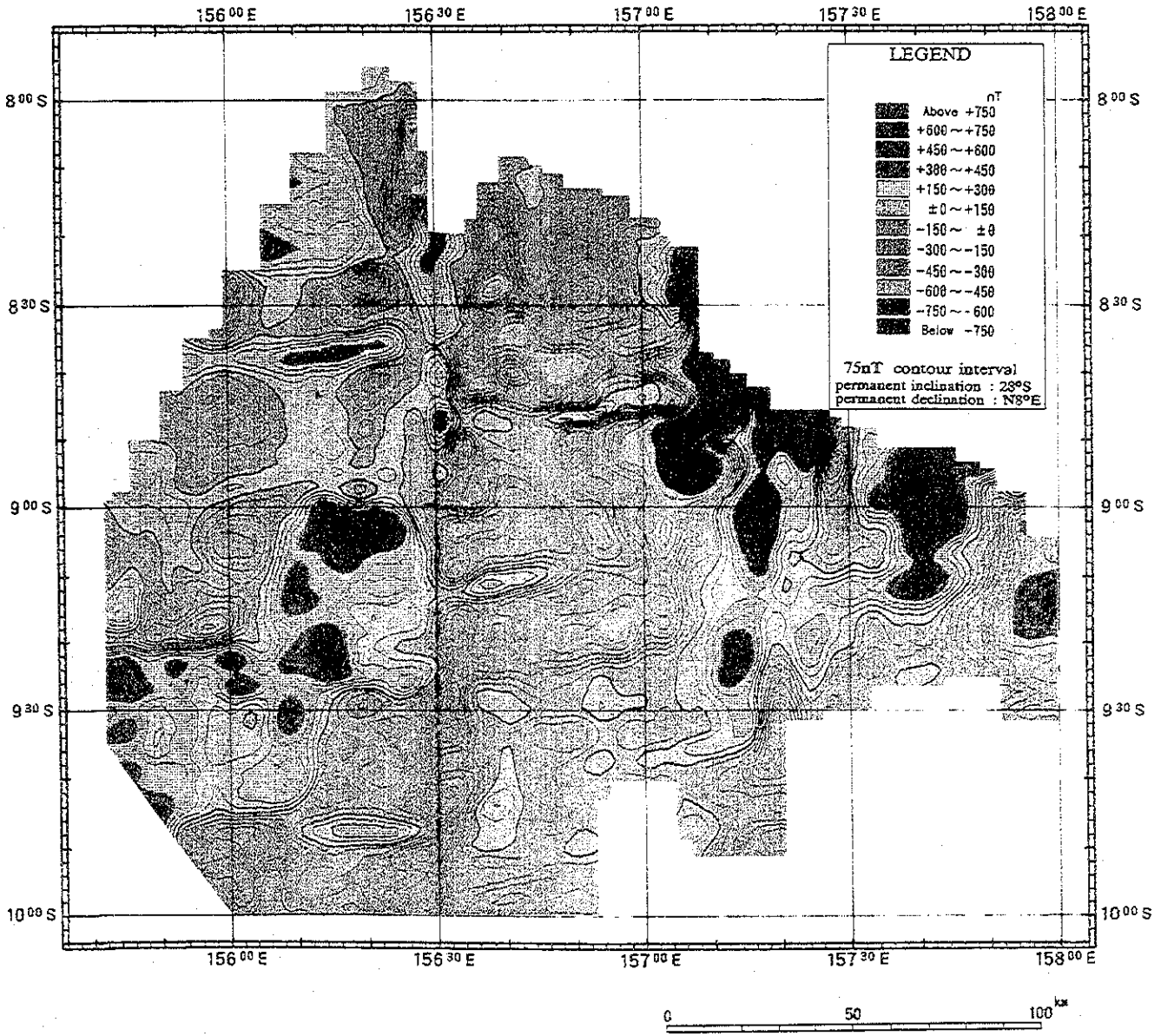


Figure 3-2-3-1 Reduction to the pole anomaly map of area 1 derived from the total magnetic force value. Contour interval is 75 nT

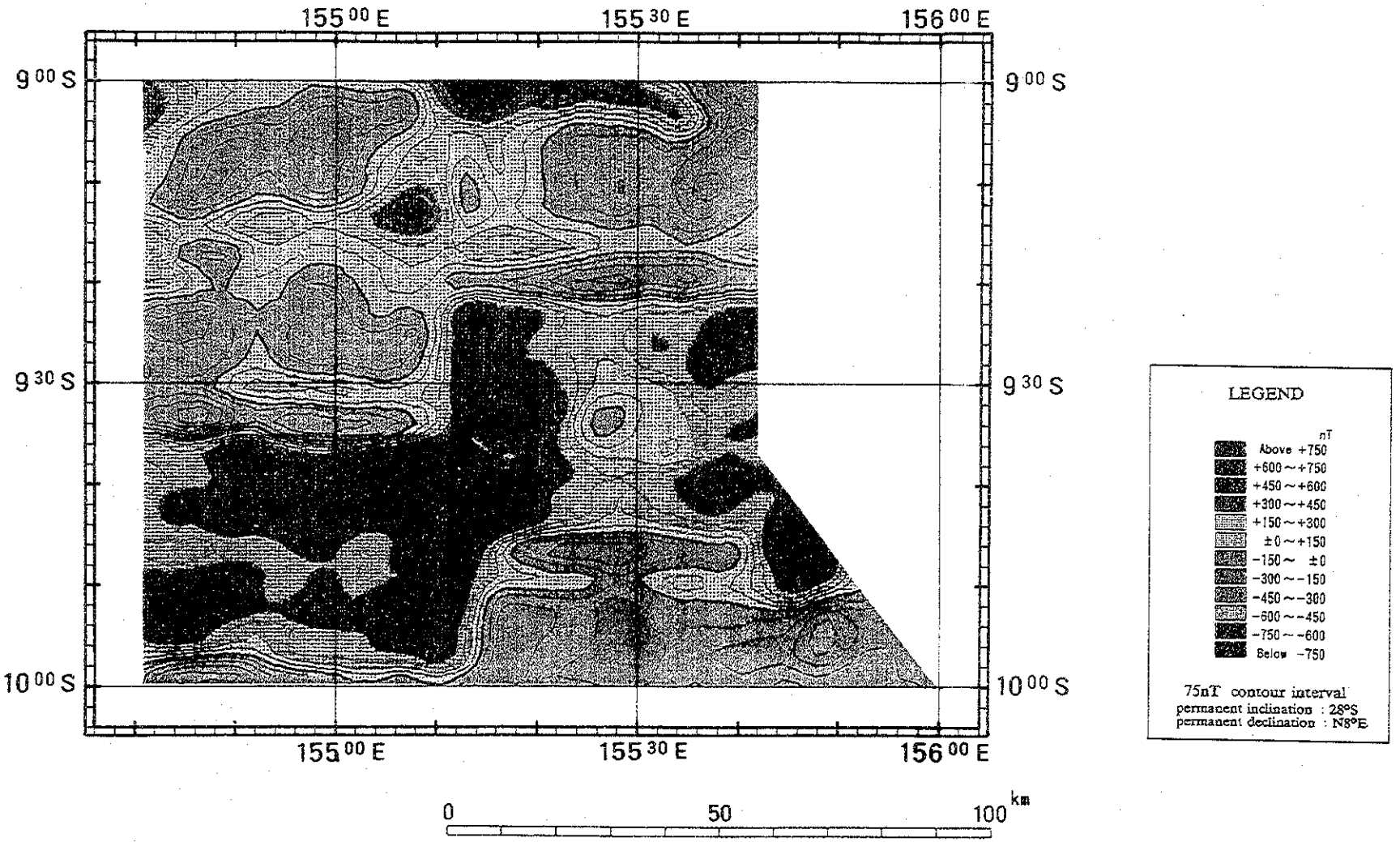


Figure 3-2-3-1 Reduction to the pole anomaly map of area 2 derived from the total magnetic force value. Contour interval is 75 nT

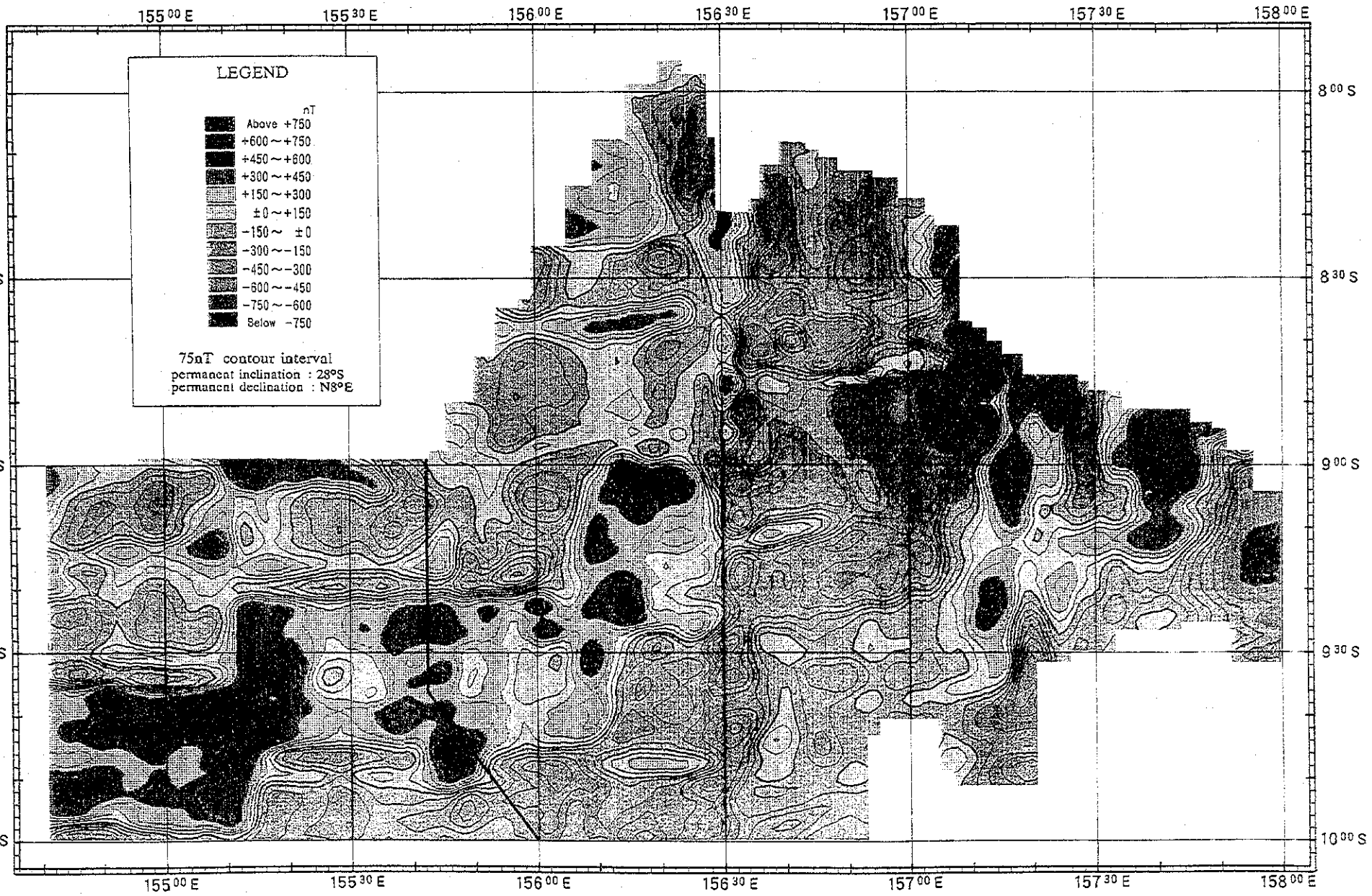


Figure 3-2-3-1 Reduction to the pole anomaly map of area 1+2 derived from the total magnetic force value. Contour interval is 75 nT

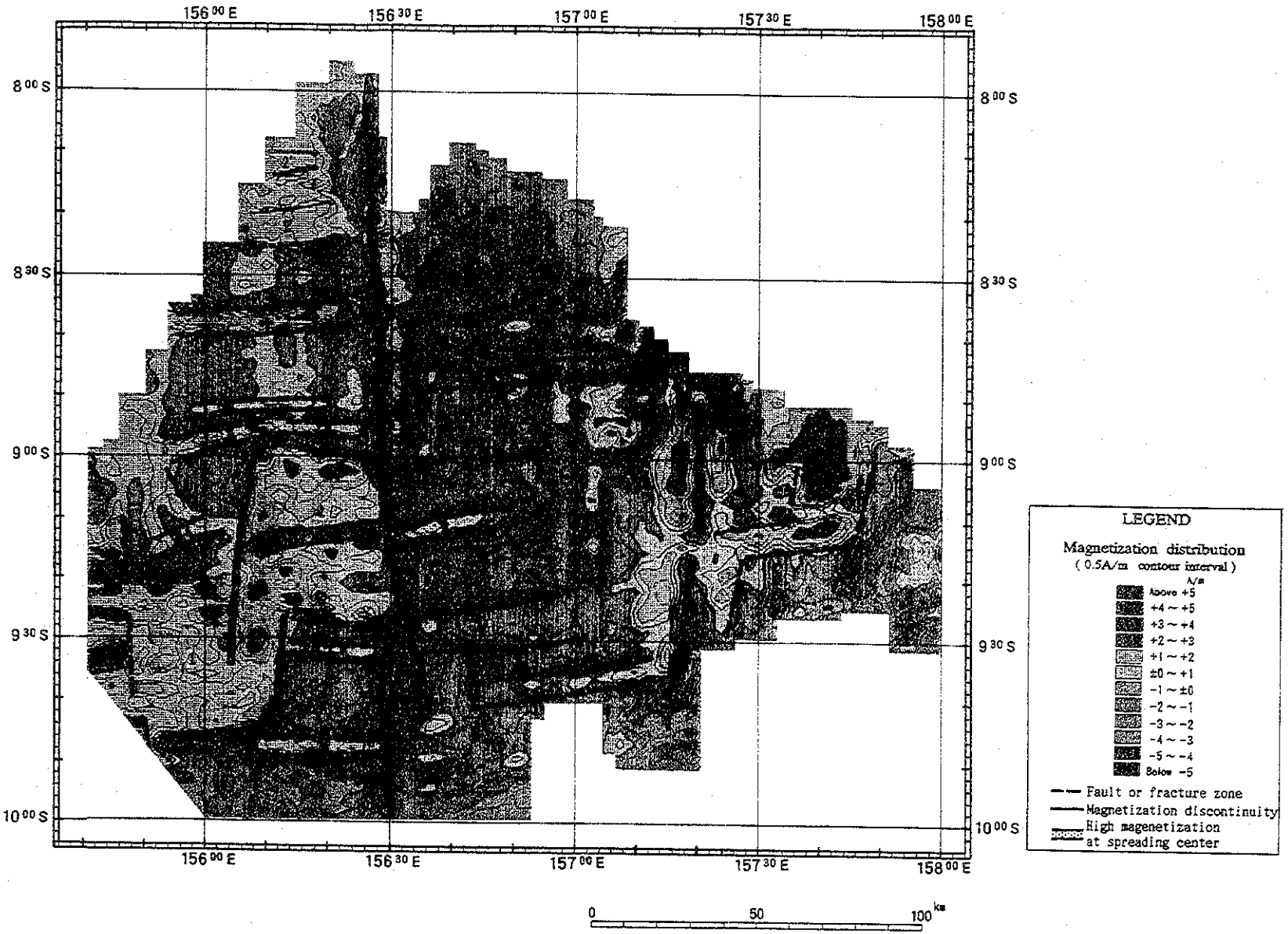


Figure 3-2-3-2 Magnetization distribution map of area 1 from three-dimensional inversion solution of gridded bathymetric and magnetic anomaly data. Contour interval is 0.5 A/m

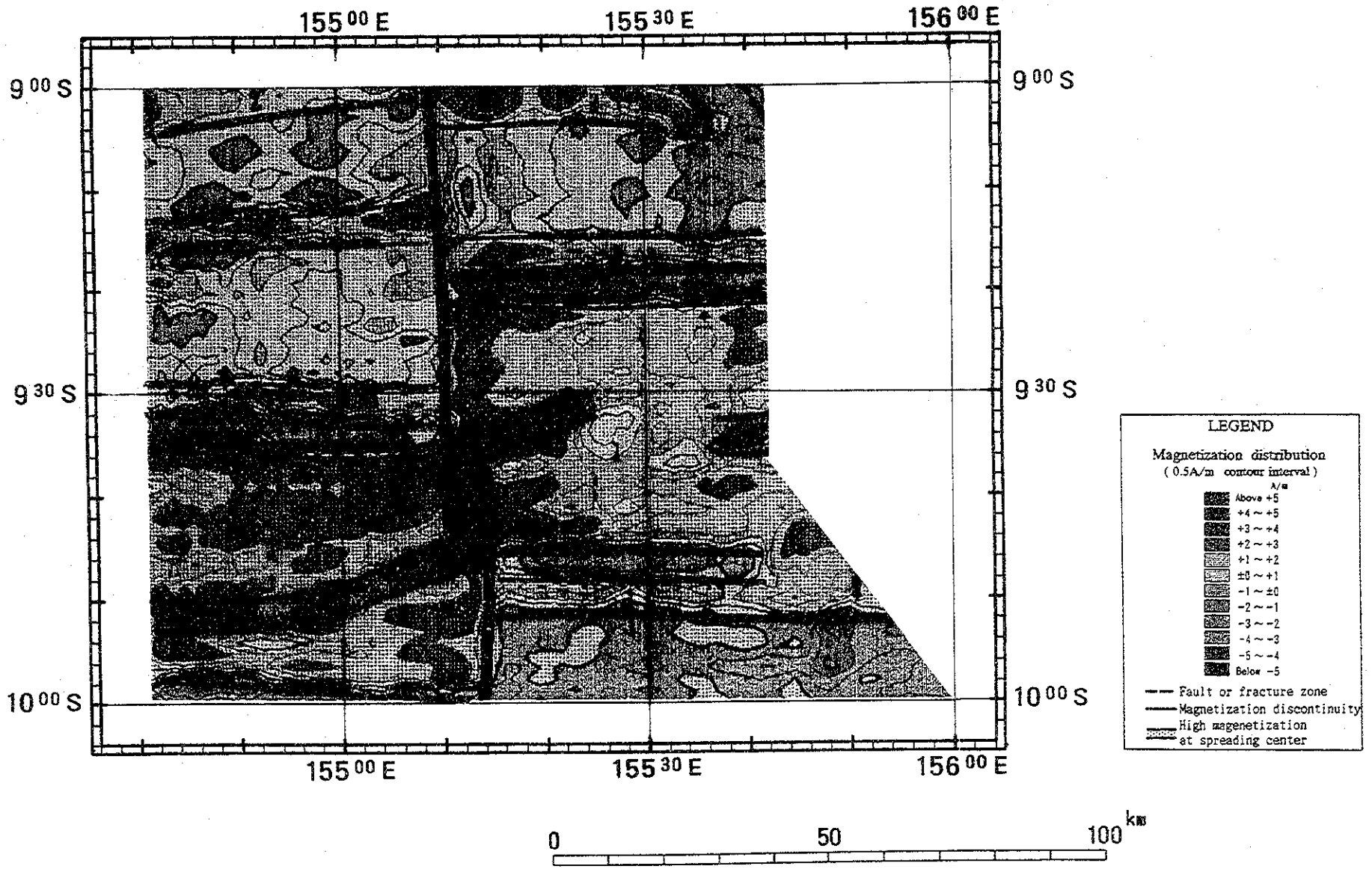


Figure 3-2-3-2 Magnetization distribution map of area 2 from three-dimensional inversion solution of gridded bathymetric and magnetic anomaly data. Contour interval is 0.5 A/m

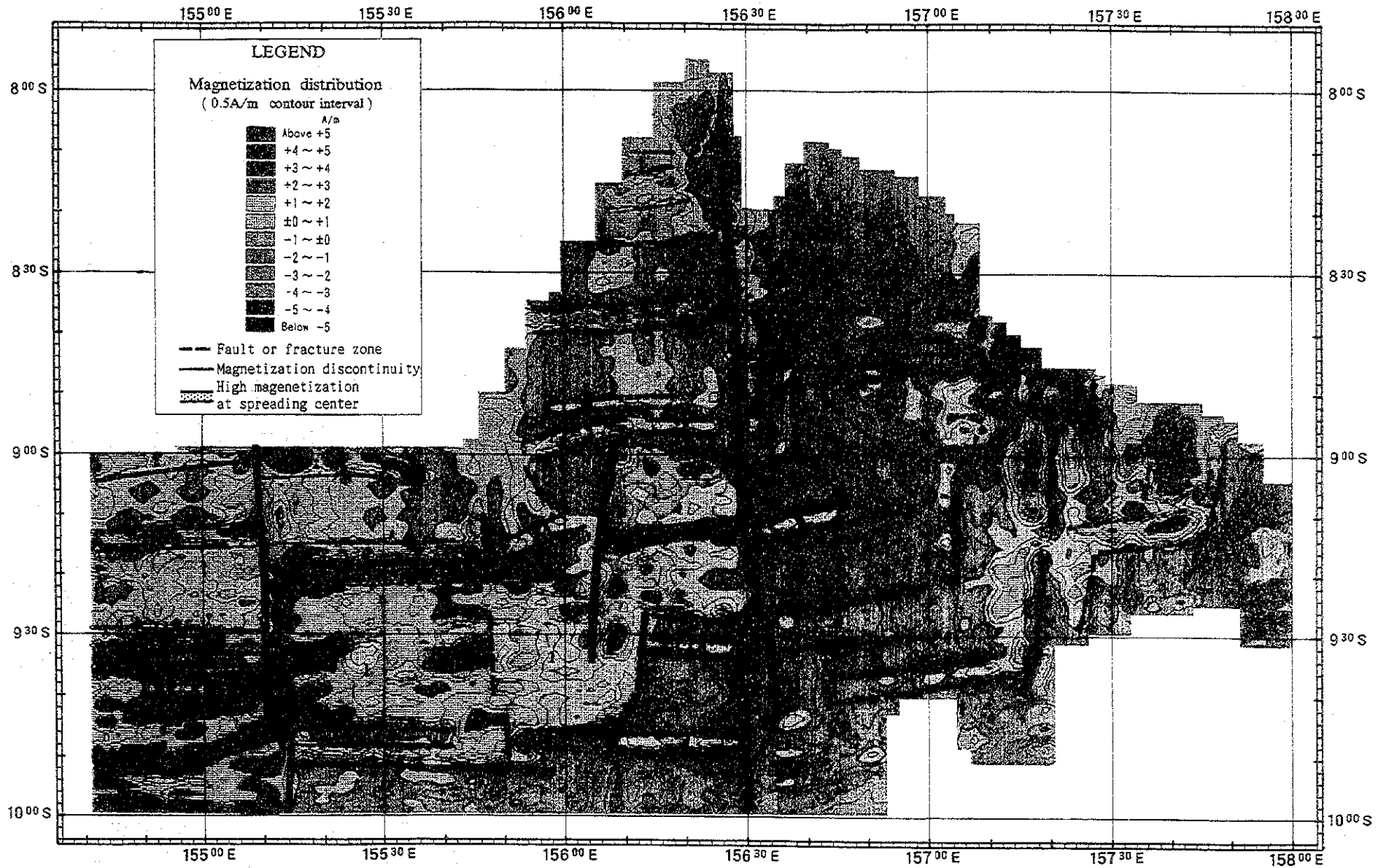


Figure 3-2-3-2 Magnetization distribution map of area 1+2 from three-dimensional inversion solution of gridded bathymetric and magnetic anomaly data. Contour interval is 0.5 A/m

Positive magnetization zone of the east-west trend is widely distributed to the west of 156° 30'E and the magnetization offsets stepwise to the south as it goes toward the west. This zone is interpreted as the Anomaly 1. Positive magnetization lineations of E-W trending are distributed symmetrically on both sides of this Anomaly 1, except where the seafloor spreading center jumps occurred. These lineations are interpreted as the Anomaly J, Anomaly 2 and Anomaly 2' respectively. Some of them are not symmetrical as a result of jumping of the seafloor spreading center in the past. A transform fault is located along 155° 10'E line and 156° 10'E line where the Anomaly 1 offsets from north to south.

If the date of the Anomaly 1 was 0.72 Ma, then the spreading rates is 7.0 cm/y at 156° 15'E, 6.7 cm/y at 155° 57.5'E, 6.2 cm/y at 155° 21.5'E and 5.7 cm/y at 155° 50'E. From which we can see that the spreading rates become slower toward the west.

The lineation east of 156° 30'E is not as clear as west of 156° 30'E.

Possibly they are divided into small blocks by many faults. In this area, Taylor (1987) suggested that the seafloor spreading center has already subducted beneath the Pacific Plate.

Negative N-S trending magnetization cutting the E-W trending magnetic structure is distributed on the 156° 30'E line. This is interpreted as the Simbo Transform Fault.

Positive magnetization zones identified with the Anomaly 2 and Anomaly 2' are distributed roughly in the direction east-west between 156° 30'E and 157° 10'E. Considering from the location of the Anomaly 2, the plates on both sides of the Simbo Transform Fault indicated about 65 km offset. Positive E-W trending magnetization is distributed around 8° 45'S, on the south of the Ghizo Ridge. Judging from this location, we interpret it not as the Anomaly J, but perhaps as a reactivated seafloor spreading center.

The Kana Keoki Seamount is located on the eastern tip of this lineation. Positive magnetization of the east-west and north-south trends are distributed at 157° 10'E and eastward. According to Taylor (1987), the Anomaly 2' exists around here. It is presumed that the Anomaly 2' segments broken into small blocks by many faults is shifted to north and south.

(2) Seamounts

The Kana Keoki Seamount is normally magnetized, but its intensity is not so high. While on the Coleman Seamount, the positive magnetization is distributed roughly eastward from the center of the seamount. It is normally magnetized and the intensity of magnetization is higher than that of the Kana Keoki Seamount.

High positive magnetization is distributed on a seamount located on the west side of the Simbo Fracture Zone, at 9° 49'S·155° 47'E.

A high peak of magnetization is located at the northern part of the seamount, and a low peak of magnetization at its southern part.

(3) Seafloor Spreading Center

High positive magnetization is distributed continuously along the seafloor spreading center but this continuity disappears between 155° 46'E and 156° 10'E.

(4) Others

Positive magnetization associated with small seamounts is distributed on the Simbo Ridge.

Positive magnetization is distributed on the Ghizo Ridge, but its intensity is lower than that of the Simbo Ridge.

High magnetization is scattered over the trench slopes at 157° 10'E and eastward.

## 3-3 Geological Structure

A geological structure map of this survey area is shown in Figure 3-3-1-1.

The geological structure of this survey area is as follows;

<Trench-Trench-Transform Triple Junction>

Crook and Taylor (1993) estimated a tripped junction at 8° 07.46'S·156° 28.7'E, NNW of the Simbo Island. A triple junction is a point where boundaries of three plates intersect. Three plates in this survey area are the Solomon Sea, India-Australian, and Pacific Plate (Fig. 3-3-1-1). Furthermore, this triple junction is comprised of the New Britain Trench, San Cristobal Trench and the Simbo Transform Fault. At present, the India-Australian Plate is subducted beneath the San Cristobal Trench, and the

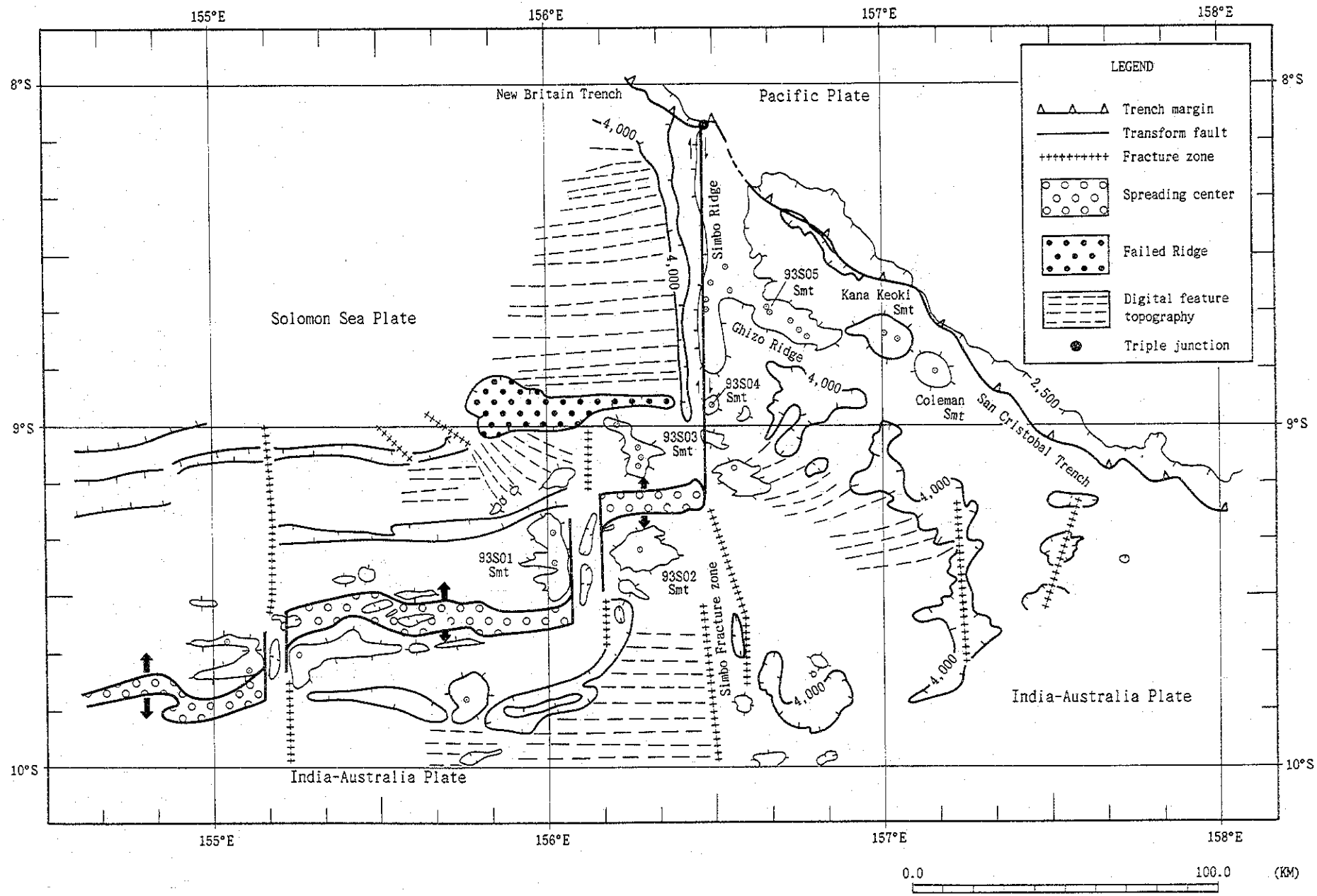


Figure 3-3-1-1 Geological structural map

Solomon Sea Plate is subducted beneath the New Britain Trench.

The Simbo Transform Fault is the line joining the eastern tip (the ending point) of the seafloor spreading center, and the above-mentioned triple junction.

East of the Simbo Transform Fault, active seafloor spreading center is nonexistent. According to Crook and Taylor (1993), on the south of the Ghizo Ridge a failed seafoor spreading center within more than 4 km-deep basins.

<Seafloor Spreading Center>

We determined that the seafloor spreading center is the valley like graben on where lied middle Brunhes-Matuyama boundary on the both sides. This spreading center is divided into three segments by two transform faults, and shifted to south at two locations, about 38 km and 26 km respectively, in a discrete step toward the west.

General characteristics of this seafloor spreading center areas follows;

(1) Occurrence depths of valley are between 3,500 and 4,600 m.

(2) The valley 5 ～ 15 km wide and with 0.5 to 1.0 km of relief. There are seamounts build on both sides or one side of the rift valley. There are small hills and small deep on the floor of the valley. Based on the results of the sampling by the GC and CB, we estimated that the thickness of the sediments in the valley is thin.

(3) The results of the magnetic survey show that the azimuth of the spreading is the south and the north. The spreading rates are between 5.7 cm/y and 7.0 cm/y if the date of the Brunhes-Matuyama boundary was 0.72 Ma (Ness et al, 1980). The spreading rates become slower toward the west.

As for the reason that the spreading rates become slower toward the west, it may have some relations with the west ward propagating rift suggested Beans et al (1992).

(4) The boundary between the seafloor spreading center and the transform faults is not clear.

(5) Its morphology resemble the rift valleys of the Mid Atlantic Ridge than the spreading axis of the East Pacific Ridge.

We describe here every segment of the spreading center.

Segment 1 (roughly along the 9° 50'S line, 155° 10'E and westward)

It is a valley with 3.5 km to 3.9 km of relief, 56 km long and 5-8 km wide. It bifurcates into two segments at around 154° 55'E and shows the morphology resembling a kind of overlapping spreading center except the short NW treding segment at around 154° 55'E. There is a potential that the northern segment becomes a failed seafloor spreading center and the southern segment grows into a new spreading center through rift propagation.

The southern segment is a continuous high magnetized band.

Segment 2 (roughly along the 9° 35'S line, between 155° 10'E and 156° 08'E)

It is a valley with 3.5 km to 4.5 km of relief, 100 km long and 5-10 km wide. There are a number of small deeps between 155° 10'E and 155° 30'E. NW trending small deeps are also located at around 155° 30'E. It has a possibility of being become a short transform fault. Or we may envision that the spreading segments at around 154° 55'E - 155° 30'E has rotated counterclockwise. High magnetized band are recognized discontinuously.

Segment 3 (roughly along the 9° 15'S line, between 156° 08'E and 156° 25'E)

It is a valley with 3.5 km to 4.5 km of relief, 30 km long and 7-11 km wide. Most of the area is occupied by small deeps. There is a continuous high magnetized band in this segment.

The E-W trending bathymetric depression lying along the 9° S line between 155° 48'E and 156° 07'E is a failed seafloor spreading center once contiguous the Segment 3.

<Transform Faults and Fracture Zones>

The transform faults are the N-S trending bathymetric depressions at the depths of deeper than 4 km, except the Simbo Transform Fault. From the both ends of these transform fault, fractured zone (weak line of old age) are stretching.

Most of the transform faults are leaky and there are ridges and the seamounts along these transform faults. For example, the Simbo Ridge lies east of the Simbo

Transform Fault. The spreading center are also accompanying ridges and seamounts.

We list here some typical transform faults and fracture zones.

(1) The fracture zone lies along the 155° 10'E line and continues from 9° 10'S to 10° 00'S (its deepest place is 4,500 m deep and its width is 6 km). The portion with the deepest water depth within the fracture zone is the transform fault. This transform fault is a N-S trending continuous high magnetized zone.

(2) The fracture zone lying along the 156° 08'E line and continues from 9° 00'S to 10° 00'S (its deepest point is 4,800 m deep and its width is 11 km). The portion with the deepest water depth within the fracture zone is the transform fault. This transform fault is a N-S trending continuous high magnetized zone.

(3) The Simbo Fracture Zone stretching from the southern tip of the Simbo Transform Fault roughly in the direction SSE (its deepest point is 4,600 m deep, more than 190 km long and less than 6 km wide). This transform fault passes between a N-S trending high magnetized zone and a N-S trending low magnetized zone.

(4) A N-S trending depression continues at the water depth of 4,500 m near 157° 15'E which implies the possibility of an old weak zone. A N-S trending high magnetized zone is located west of this fracture zone.

Furthermore, the results of magnetic survey show that there are a number of fracture zones and faults in addition to those expressed in the tectonic map, the east of the Simbo Transform Fault and Fracture Zone.

<Trenches>

We have draw a landward (Solomon Islands) boundary of the New Britain and San Cristobal Trench in the tectonic map.

(1) The San Cristobal Trench trend is irregular as it has several reentrants and cups (salients). These features have relation to the existence of thrusts and landslides (Honza, 1988 and Crook and Taylor, 1993).

(2) Small, high magnetized zones are found here and there on the trench landward slopes.

(3) The water depth of the trench becomes 3,050 m near the saddle of the Kana Keoki and Coleman Seamounts.

(a) The piedmonts (deeper than 3,000 m) of the north-eastern fabric of the Kana Keoki and Coleman Seamounts disappeares at around this trench.

(b) The width of the trench landward slope is narrow. Angles of the trench landward slope and seaward slope are approximately 5° -13° and 5° respectively.

The area between (a) and (b) is a flat seafloor with partly slot-like ditches.

<Digital feature of Ridge and Valleys>

Series of E-W trending parallel ridges and valleys are arranged in a digital feature in the north and south of the area on the west of the Simbo Transform Fault and Fracture Zone. On its east, from 9° 20'S and southward, ENE trending ridges and valleys are arranged like a comb.

<Ridges and Seamounts>

Prominent seamounts and ridges in this survey area include the followings;

(1) Water depths of the summits of seamounts and ridges in the vicinity of the transform faults and the seafloor spreading center is between 1,800 m and 2,400 m. These seamounts and ridges stretch gently, in a digital shape, in the direction east-west. The FDC survey shows that the rock of these seamounts and ridges is mainly composed of basalt. All of these seamounts and ridges are normaly magnetized.

(2) A seamount is located at 9° 50'S·155° 45'E. This seamount is located around the Brunhes-Matuyama boundary, but is normaly magnetized with high magnetization.

(3) There are the N-S trending Simbo Ridge and the N-W trending Ghizo Ridge. The Kana Keoki Seamount and Coleman Seamount are located in the southeast of the Ghizo Ridge.

These ridges and seamounts, on the Australian plate side, are dredged island arc type rocks. The magnetization of the Simbo Ridge is higher than that of the Ghizo Ridge.

(4) The Kana Keoki Seamount is stretched in the direction of the Ghizo Ridge. The northern part of the seamount has slipped laterally in the WSW direction. The piedmont (deeper than 3,000 m) on the northeastern part of the seamount has disappeared. Basalt, andesitic rock, white argillized rock and siliceous rock were dredged from this seamount. This seamount is positively magnetized and its intensity of magnetization is lower than that of the Coleman Seamount.

(5) A horseshoe shape peak is identified on the summit of the Coleman Seamount, which indicates a potential of the existence of a caldera. The figure of the seamount is cone but the trenchward piedmont (deeper than 3,000 m) has disappeared. Island arc type rocks were dredged from this seamount.

(6) As the present active Kavachi Volcano, located on the trench landward slope at the north-eastern survey area, we, therefore, could not carry out the survey. The characteristics of the Kana Keoki Seamount, Coleman Seamount and Kavachi Volcano is the near-trench magmatism (Taylor 1987).

# Chapter 4. Regional Geochemical Survey

## 4-1 Outline

With the objective of making a survey on present hydrothermal activities and traces of past hydrothermal activities through the geochemical method and, at the same time, obtaining background data for this purpose, we collected submarine sediments, roughly evenly, from the survey area.

Samples were collected from a rectangular area spreading in 8° 15'S～10° 00'S・155° 45'E ～ 158° 00'E, as shown in Figure 2-7-1. Sampling points were arranged on the grid established at intervals of 30 minutes latitude and longitude respectively and its center.

Initially, we had planned to collect samples at 24 points, but we failed to collect sediments at 3 points (we collected rocks at one point out of the three), so we actually collected sediment at 21 points.

As for the sampling method, we employed a gravity corer and a large corer to collect columnar samples. The length of the core-tube is 2 m or 4 m. Deformation of the tip of the corer bit was recognized when the bit tip hitted a rock mass.

The sampling points are indicated by 93 (the latter two figures of the Christian Era) + S (the first letter of SOPAC) + R (the first letter of Regional) + GC or LC (the sampler: GC represents Gravity Corer and LC represents Large Corer) + serial numbers in two figures in order of sampling (including the re-try in the case when the initial sampling failed). In this cruise, the first sampling point is represented by "93SRGC01" and the last sampling point by "93SRGC26".

Data of location, water depth, equipment used and length collected on the each sampling point are shown in Appendix Table 1.

Collected columnar samples were sketched in geological columnar sections and a part of the half cores were sampled for laboratory tests such as chemical analysis and powder X-ray diffraction tests, and the remaining half cores were preserved.

## 4-2 Properties of the Collected Samples

### 1) Muddy Substances

Collected samples were classified mainly according to their color tones and grain sizes. The "Munsell Soil Color Charts" were used for the classification of the color tones and the Wentworth Grain Size Scale (1922) was used for the classification of the grain sizes. The color tones of the samples are mainly composed of the 10YR ~ 2.5YR series (brown series) and 5Y series (olive series) of the "Munsell Soil Color Charts". The grain sizes of the samples are mainly composed of clay and, partly, of the silt and coarse-grained sand under the Wentworth Grain Size Scale (1922). As a result of the grain size analysis of a part of the samples collected (37 samples/4 points), that the median diameter and mean diameter of these bottom materials are found to within the range of micro-grained ~ medium grained silt. The results of this test will be described later.

The sampling results of the regional survey classified mainly by the above-mentioned standards are shown in Figure 4-2-1-1 as a schematic diagram.

The main components of the muddy substances are clay, calcareous shells of foraminifera and clastic minerals.

These three substances are always contained in the muddy substances, though the ratio of them varies. Besides these main components, a very small quantity of volcanic glass as well as microfossils of radiolaria, diatoms and sponge spicules are commonly contained. Authigenic minerals are not recognized, or, if any, at extremely rare intervals.

It is difficult to identify details of the clay with a microscope because the clay is extremely fine-grained (smaller than several $\mu$m). We presumed that the difference of color tones between the 10YR ~ 2.5YR (brown) series and the 5Y (olive) series - is mainly caused by this clay as there is no other traceable component in most cases. Sometimes, clay coagulates around calcareous shells of foraminifera or clastic minerals and becomes insoluble substance.

The color of the calcareous shells of foraminifera is white. Their sizes are generally between 50 $\mu$m and 1 mm, but the bigger shells can be observed only as fragments when observed under the microscope. The content of calcareous shells of foraminifera in the muddy substances varies diversely but, in most cases, the content is less than 10% when observed under the microscope. Rarely, they enrich densely on

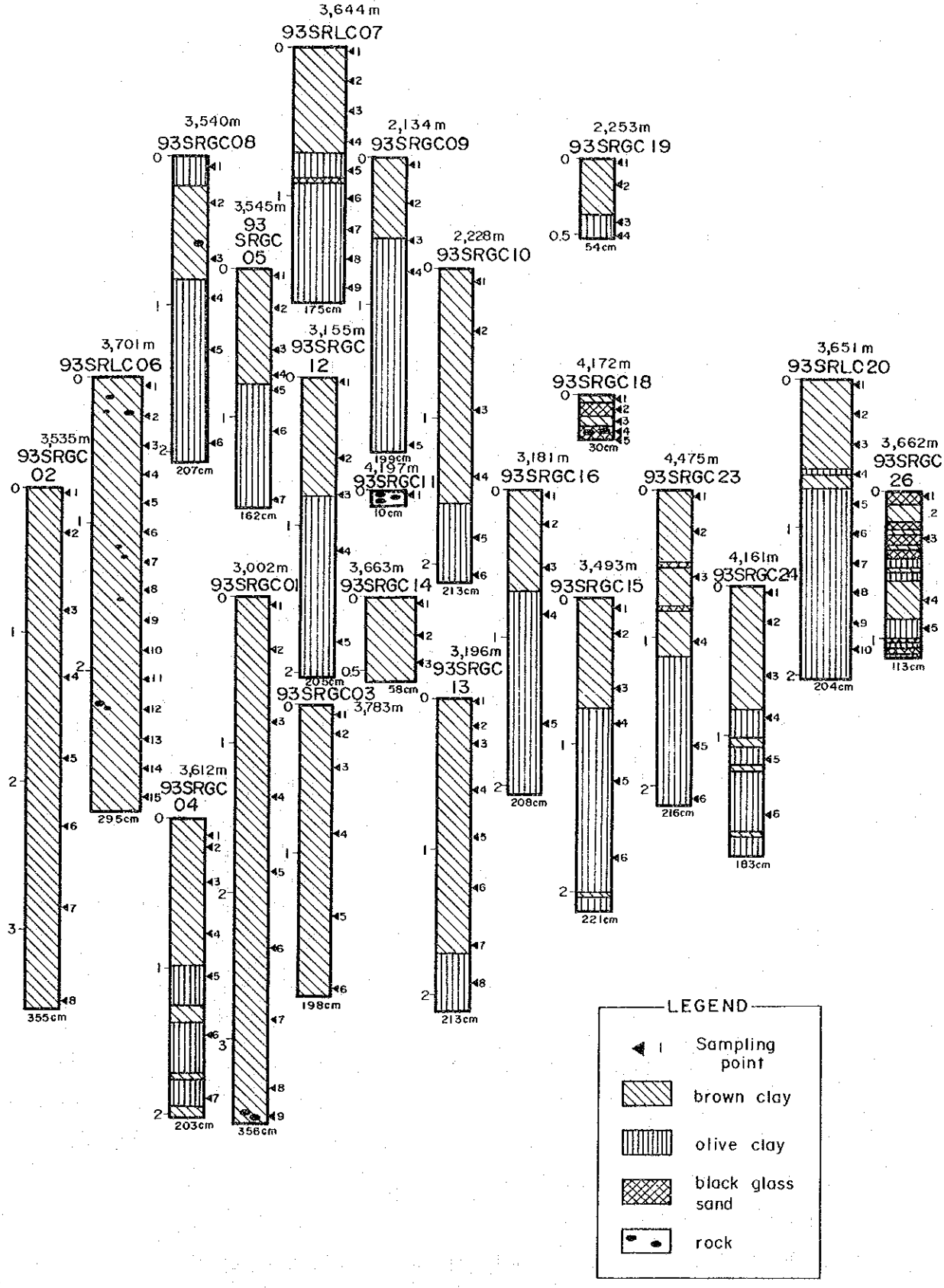


Figure 4-2-1-1 Schematic Drawings of Sampling Results Obtained from Regional Geochmical Survey

the submarine surfaces and shallow parts. And, sometimes, horizons that can be regarded as foraminiferaous sand are identified. Most of the array patterns of the chambers of foraminifera fossils are trochoidal spirals ~ planispiral ~ in the form of two rows. Most of them are, therefore, considered to be falling under the superfamily of the Globigerinacea of the Planktonic Foraminifera. Furthermore, with the objectives of estimating the age and rate of sedimentation as well as the paleoenviroment of the sediments, vertical and continuous sampling for four points of the regional survey, and the identification of foraminifera fossils contained in these samples were carried out. As a result, the age of the sediments is estimated as roughly younger than 0.3 Ma and the rate of sedimentation is faster than 2-3 mm/ka. The details of these tests and results will be described later.

Among clastic minerals, plagioclase, quartz, amphibole and pyroxene are commonly contained, though a small amount, in most of the muddy substances. Quartz generated by the process of divitrification of felsic volcanic-glass is also recognized in many samples. The plagioclase does not give a sign of zoning. Most of the plagioclase and quartz present the morphology of the fragmented allotriomorph but the amphibole, characterized by its strong pleochroism of brown to green, present a long piller-shaped form close to the fragmented idiomorph. The sizes of these clastic minerals are generally smaller than 50 $\mu$m. Opaque minerals are also generally contained, although a small amount, in most of the muddy substances. Macroscopically, sediments containing much opaque minerals in abundance assume a strong color tone of gray. The occurrence of filling up the shell chambers of foraminifera fossils or the bubbles of volcanic glass or the cavities of sponge spicules with opaque minerals is also recoginzed. These opaque minerals might be generated secondarily after the sedimentation. The sizes of the opaque minerals are generally about 10 $\mu$m.

Volcanic glass identified in this sea area's sediments is generally a very small quantity when observed under the microscope but some of its fine-grained volcanic glass could be as fine as the size of clay. So, we estimate that the volcanic glass exists quite commonly in the sediments. Volcanic glass observed under the microscope can be classified into two categories, i.e. felsic glass and mafic glass. It is estimated that the quantity of felsic glass is relatively greater than that of mafic glass when observed under the microscope. The mafic glass tends to form a thin layer practically composed of itself. The felsic glass assumes transparent ~ white translucent colors. The size of felsic glass is generally smaller than 50 $\mu$m. The

mean diameter of felsic glass is somewhat larger than that of mafic glass. A morphological feature of the felsic glass in this area is that it has a structure with a number of spheroidal bubbles. On the other hand, the mafic glass assumes a brown color. Its size is several $\mu$m and 50 $\mu$m, its mean value is about 20 $\mu$m. Most of it is small plate-shaped fragments with a small quantity of bubbles inside.

Siliceous microfossils such as radiolaria, diatoms and sponge spicules are commonly observed in the survey area, though their quantity is very small. The size of radiolaria is roughly smaller than 100 $\mu$m and there are plenty of Euchitonia which indicate the tropical community. But most of them are fractured and in a bad state of preservation. Diatoms are round, centric diatoms with diameters of several $\mu$m to 50 $\mu$m, but pennate diatoms are not recognized. Sponge spicules are observed as several $\mu$m wide hollow pipes, but sponge spicules amounting to hundreds of $\mu$m are rarely found. They are in a slightly bad state of preservation.

Altered pumice (with diameters from 1 cm to 2 cm) is observed macroscopically off and on in the sediments composed of the above-mentioned components.

The most remarkable vertical variation seen in the sediments of this area is its color tones. The general rule that the 10YR $\sim$ 2.5YR series (brown series) sediments will be distributed relatively above the 5Y series (olive series) sediments is materialized at almost every point. The boundaries of the two series are irregular. Sometimes, the boundary is clearly divided by a thin, semiconsolidated layer but, sometimes, the two series show a transitional relationship. There is no clear difference between the two series as to the quantitative ratio of the components.

There is no relevancy between the boundary depths of the 10YR series sediments and 5Y series sediments (the lower basal-plane depths of the 10YR $\sim$ 2.5YR series sediments) and the water depths (Figure 4-2-1-2). But this boundary depths show a tendency to become deeper as the locations leave the trenches (Figure 4-2-1-3). All the cores collected from the sampling points of 93SRGC01, 93SRGC02, 93SRGC03 and 93SRLC06, the south-western part of the survey area, are the 10YR series sediments from the top to the bottom. It is considered that the brown series sediments will show that they are under the oxidizing environment and the olive series sediments are under reducing environment.

As for the horizontal variation seen in the sediments of this area, such tendencies as a decrease in fossil shells of foraminifera and a increase in volcanic

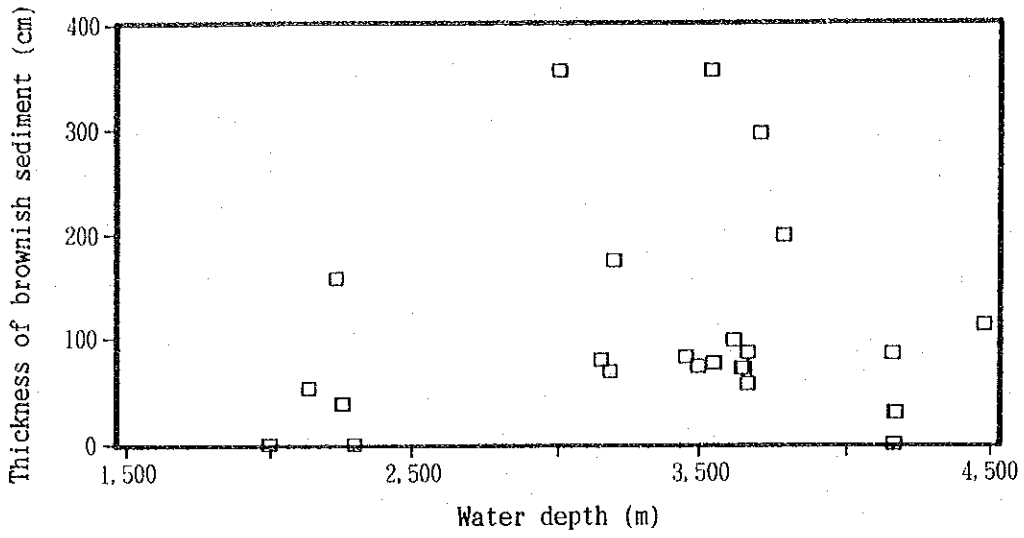


Figure 4-2-1-2 Relationship of water depth of sampling sediment and depth of brownish sediment from sea bottom

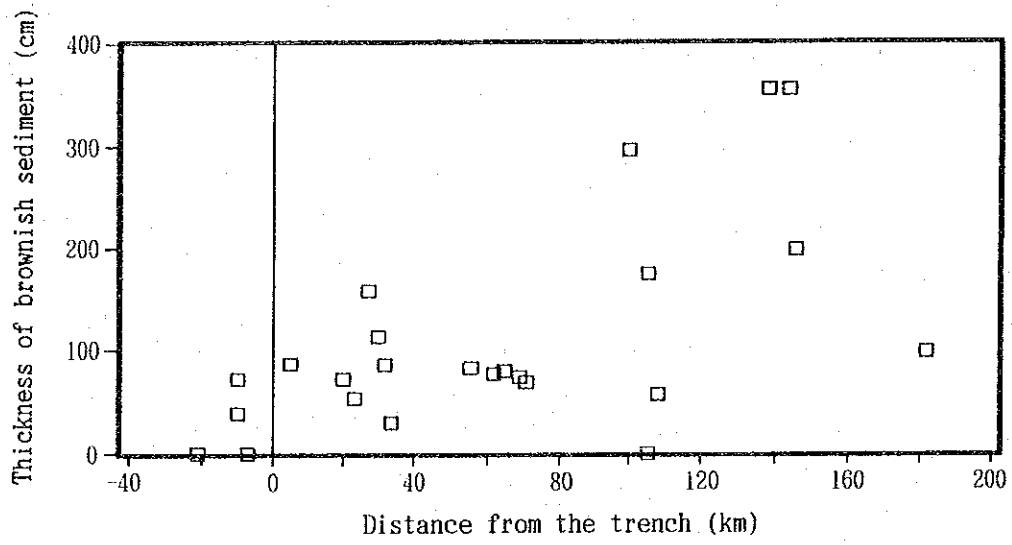


Figure 4-2-1-3 Relationship of distance from the trench and depth of brownish sediment from sea bottom

glass at the north-eastern side of the survey area (especially at 93SRGC18, 93SRGC19, 93SRLC20, 93SRGC23, 93SRGC24 and 93SRGC26) are recognized macroscopically and microscopically.

<Discrimination of Microfossils in the Seafloor sediments>

With the objective of estimating the date of sediments and the rate of sedimentation, as well as the paleoenvironment, vertical and continuous sampling was conducted at four points (i.e. 93SRLC06, 93SRLC07, 93SRLC14 and 93SRLC20) selected from the regional survey's sampling points. And the discrimination of foraminiferous fossils containing in the samples collected from these four sampling points was conducted. The samples were collected at intervals of 20 cm from the upper layer (sea-bottom surface) of the sampling points. The number of samples are 15 samples from 93SRLC06 (-1M to -15M), 9 samples from 93SRLC07 (-1M to -9M), 3 samples from 93SRLC14 (-1M to -3M) and 10 samples from 93SRLC20 (-1M to -10M).

The samples were washed with water on a 200-mesh (74 $\mu$m) screen, dried by a thermostatic dryer and divided by a divider so as to make between 200 and 300 individuals. The samples are abundant in foraminiferous fossils but radiolarian fossils are hardly contained. Extracted foraminiferas can be classified into planktonic foraminiferas and benthic foraminiferas. As for the planktonic foraminiferas, only the individuals larger than 80-mesh (150 $\mu$m) were undergone the discrimination of species and the measurement of numbers.

The results of the analysis tell that the greater part of the foraminiferas are planktonic foraminiferas and benthic foraminiferas are few.

Blow's (1969) fossil zone classification was applied for the analysis of planktonic forminiferas and each species' index datum and its geological time are based on the geochronologic classification of Berggren et al. (1985). As these index datum are related to the communities of the low-latitude areas, so we think they can be applied to this survey area. The fossil zone classification and their index surfaces were established by Parson et al. (1992). However, index species such as *Globorotalia crassaformis viola, Globorotalia crassaformis hessi, Pulleniatina finalis* and so on did not occur from the samples analized, so it is difficult to discuss the correlation of fossil zones for those occurred after the latter period of the Pleistocene Epoch (especially from the latter term of the N22 zone to N23 zone). We will discuss various aspects including a method of determining the geological time

based on the spiral direction of the species of *Pulleniatina* genus (Saito, 1976) and *Pulleniatina* datum & *Globoquadrina conglomerata* datum pointed out by the study of the Pacific Equatorial piston cores conducted by Takayanagi et al. (1979) in the following paragraph. Major datum and their estimated ages counting from the lower layers are as follows:

- *Pulleniatina* datum (the highest horizon on which the spiral directions of this genus turn from counterclockwise to clockwise counting from the lower layers to upper layers) (L1 of Saito, 1976; Takayanagi et al., 1979): about 0.74 Ma
- *Globorotalia tosaensis* (top) datum (Oda, 1975, 1977; Thompson, 1977): 0.6 Ma
- *Globoquadrina conglomerata* (base) datum (Takayanagi et al., 1979): about 0.55 Ma
- *Globigerinella calida calida* (base) datum (Blow, 1969): 0.3 Ma
- *Globogerinoides ruber* with pink shells (top) datum (Thompson et al., 1979): 0.12 Ma

Now we will describe the state of preservation and estimated ages of the planktonic and benthic foraminiferous fossils classified by each sampling point. Planktonic foraminifereous specimens clearly indicating the resedimentation in different ages are not identified, but resedimentary individuals are identified in a part of the benthic foraminiferous fossils. The typical scanning microphotographs of planktonic foraminiferous fossils are shown in Fig. 4-2-1-4.

- 93SRLC06

The detection results of planktonic foraminiferous fossils from this core's 15 samples are shown in Table 4-2-1-1, and the detection results of benthic foraminiferous fossils are shown in Table 4-2-1-2.

The preservation state of the planktonic foraminiferous fossils obtained from this core is not good. The lower half of the core is especially bad. *Globorotalia truncatulinoides* occurs in the sample (-15M) taken out from the lowest part of the core, but *Globorotalia tosaensis* does not occur in this part, so it is considered to belong to the latter period of the Pleistocene Epoch. Furthermore, from the fact that *Globigerinella calida calida* occurs in the samples taken out from the upper part of -14M, it is considered as indicating the

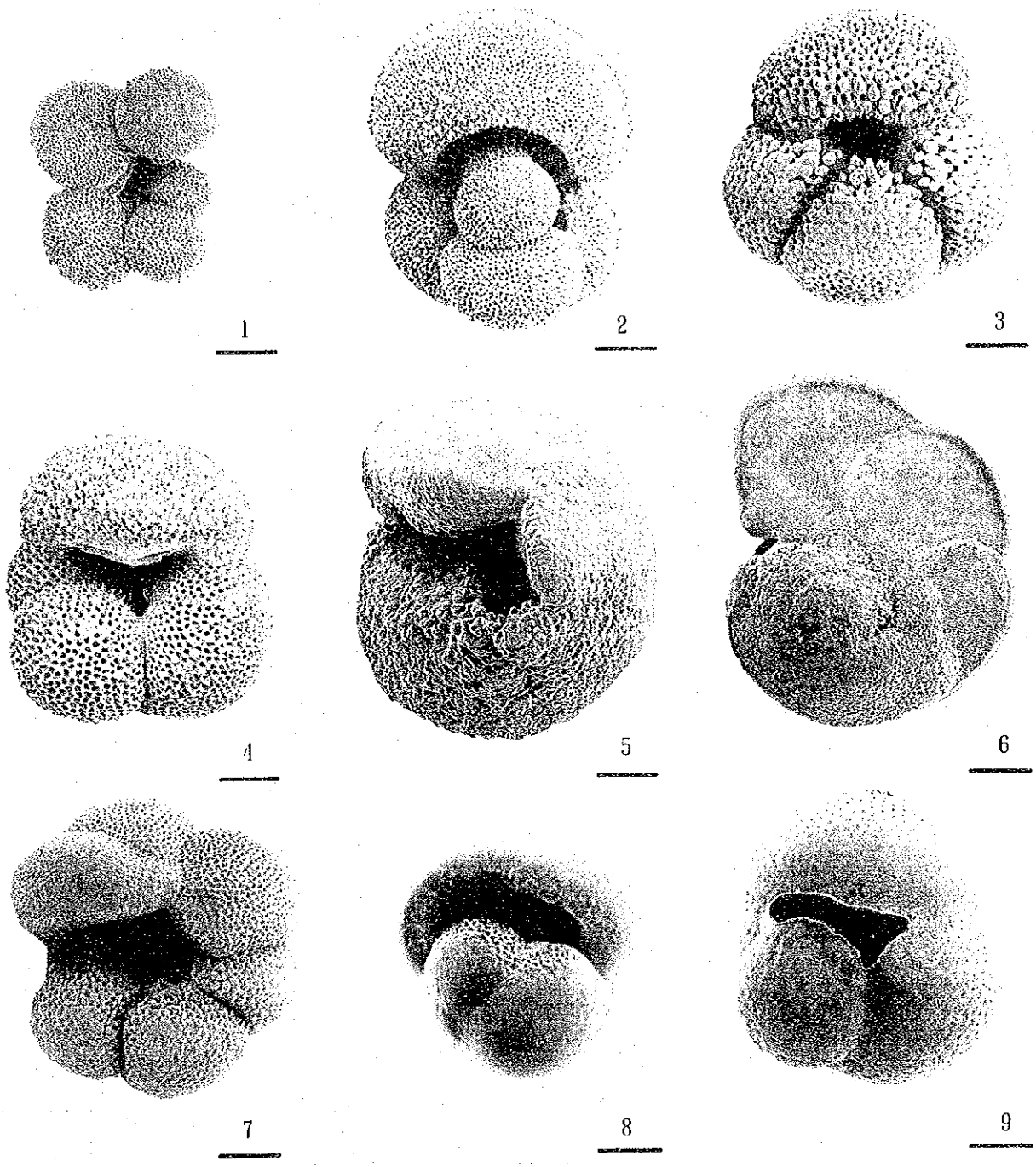


Scale Bars:100 μm

1. *Globigerinella calida* (Parker) (93-RLC20-9M) umbilical view
2. *Globigerinella aequilateralis* (Brady) (93-RLC20-9M) side view
3. *Globigerinoides conglobatus* (Brady) (93-RLC20-4M) umbilical view
4. *Globoquadrina conglomerata* (Schwager) (93-RLC06-7M) umbilical view
5. *Globorotalia truncatulinoides* (d'Orbigny) (93-RLC06-11M) umbilical view
6. *Globorotalia tumida* (Brady) (93-RLC20-1M) spiral view
7. *Neogloboquadrina dutertrei* (d'Orbigny) (93-RLC20-9M) umbilical view
8. *Pulleniatina obliquiloculata* (Parker and Jones) (93-RLC20-4M) side view
9. *Sphaeroidinella dehiscens* (Parker and Jones) (93-RLC20-1M) umbilical view

Figure 4-2-1-4 Species of the Typical Foraminifera Fossils (Planktonic Foraminifera)

Table 4-2-1-1 Stratigraphic distribution of planktonic foraminifera from cores (93SRLC06, 07, 14, 20)

93SRLC06

| preservation | 15M P | 14M P | 13M VP | 12M VP | 11M P | 10M P | 9M P | 8M P | 7M M | 6M M | 5M M | 4M M | 3M M | 2M M | 1M M |
|---|---|---|---|---|---|---|---|---|---|---|---|---|---|---|---|
| Candeina nitida | 0 | 0 | 0 | 0 | 0 | 0 | 0 | 0 | 0 | 0 | 0 | 0 | 0 | 0 | 0 |
| Globigerina bulloides | 0 | 2 | 2 | 0 | 7 | 3 | 0 | 0 | 9 | 2 | 7 | 1 | 2 | 13 | 8 |
| Gna. falconensis | 1 | 1 | 1 | 0 | 0 | 0 | 0 | 0 | 0 | 0 | 0 | 0 | 0 | 0 | 0 |
| Gna. rubescens | 0 | 0 | 0 | 0 | 0 | 0 | 0 | 0 | 0 | 0 | 0 | 0 | 0 | 0 | 0 |
| Globigerinella aequilateralis | 8 | 14 | 3 | 3 | 6 | 19 | 6 | 4 | 20 | 18 | 11 | 13 | 16 | 33 | 34 |
| Gnl. calida | 0 | 2 | 0 | 0 | 5 | 0 | 1 | 1 | 1 | 5 | 1 | 0 | 1 | 2 | 10 |
| Gnl. digitata | 0 | 0 | 0 | 0 | 1 | 2 | 1 | 2 | 2 | 0 | 0 | 0 | 0 | 0 | 0 |
| Globigerinita glutinata | 0 | 4 | 3 | 0 | 17 | 4 | 0 | 0 | 21 | 20 | 9 | 4 | 7 | 15 | 24 |
| Globigerinoides conglobatus | 12 | 5 | 0 | 2 | 5 | 12 | 16 | 6 | 14 | 32 | 24 | 10 | 5 | 2 | 11 |
| Gds. elongatus | 0 | 0 | 0 | 0 | 1 | 0 | 0 | 0 | 2 | 1 | 1 | 0 | 0 | 0 | 2 |
| Gds. ruber | 2 | 13 | 3 | 1 | 12 | 26 | 0 | 1 | 30 | 63 | 39 | 24 | 28 | 18 | 75 |
| Gds. sacculifer | 2 | 9 | 1 | 0 | 7 | 7 | 1 | 1 | 9 | 21 | 16 | 4 | 8 | 9 | 20 |
| Gds. trilobus | 5 | 13 | 5 | 1 | 12 | 38 | 0 | 1 | 37 | 35 | 25 | 13 | 16 | 8 | 20 |
| Gds. tenellus | 0 | 0 | 0 | 0 | 0 | 0 | 0 | 0 | 0 | 0 | 0 | 0 | 0 | 0 | 1 |
| Globoquadrina conglomerata | 1 | 2 | 1 | 0 | 2 | 0 | 0 | 0 | 2 | 2 | 1 | 1 | 1 | 0 | 0 |
| Globorotalia bermudezi | 0 | 0 | 0 | 0 | 0 | 0 | 0 | 0 | 0 | 0 | 0 | 0 | 0 | 0 | 0 |
| Grt. crassaformis | 9 | 8 | 32 | 11 | 11 | 12 | 9 | 6 | 12 | 5 | 3 | 2 | 2 | 1 | 1 |
| Grt. hirsuta | 0 | 0 | 0 | 0 | 0 | 0 | 0 | 0 | 0 | 1 | 1 | 0 | 0 | 1 | 0 |
| Grt. inflata | 0 | 2 | 0 | 0 | 0 | 0 | 0 | 0 | 2 | 0 | 0 | 1 | 4 | 0 | 0 |
| Grt. scitula | 0 | 0 | 0 | 0 | 0 | 0 | 0 | 0 | 2 | 1 | 0 | 2 | 0 | 0 | 0 |
| Grt. menardii | 36 | 38 | 34 | 37 | 49 | 65 | 68 | 22 | 72 | 60 | 38 | 23 | 19 | 19 | 14 |
| Grt. truncatulinoides | 10 | 8 | 4 | 2 | 25 | 53 | 3 | 5 | 15 | 12 | 4 | 5 | 2 | 5 | 1 |
| Grt. tumida | 16 | 8 | 70 | 46 | 28 | 15 | 28 | 32 | 3 | 1 | 0 | 0 | 3 | 8 | 2 |
| Grt. ungulata | 0 | 0 | 0 | 0 | 0 | 0 | 0 | 0 | 0 | 0 | 0 | 0 | 1 | 0 | 0 |
| Neogloboquadrina dutertrei | 147 | 77 | 42 | 55 | 87 | 86 | 73 | 62 | 105 | 92 | 45 | 89 | 56 | 59 | 39 |
| Orbulina universa | 0 | 0 | 0 | 0 | 0 | 2 | 1 | 1 | 0 | 5 | 0 | 0 | 0 | 0 | 1 |
| Pulleniatina obliquiloculata | 32 | 37 | 42 | 39 | 39 | 70 | 63 | 39 | 34 | 33 | 19 | 32 | 22 | 25 | 20 |
| Sphaeroidinella dehiscens | 1 | 0 | 1 | 2 | 1 | 4 | 5 | 0 | 2 | 1 | 0 | 0 | 1 | 0 | 1 |
| PLANKTONI FORAM. TOTAL | 282 | 243 | 244 | 199 | 315 | 418 | 275 | 183 | 394 | 410 | 244 | 224 | 194 | 218 | 284 |
| BENTHIC FORAMINIFERA | 11 | 2 | 41 | 59 | 5 | 11 | 14 | 21 | 13 | 0 | 2 | 4 | 4 | 0 | 3 |

93SRLC07

| 9M G | 8M G | 7M M | 6M G | 5M G | 4M M | 3M M | 2M G | 1M M |
|---|---|---|---|---|---|---|---|---|
| 0 | 0 | 0 | 0 | 0 | 0 | 0 | 0 | 0 |
| 13 | 14 | 10 | 13 | 17 | 16 | 20 | 28 | 5 |
| 2 | 1 | 0 | 0 | 0 | 0 | 0 | 0 | 1 |
| 0 | 1 | 0 | 0 | 0 | 1 | 0 | 0 | 0 |
| 29 | 20 | 11 | 12 | 6 | 9 | 36 | 65 | 57 |
| 1 | 3 | 3 | 6 | 4 | 3 | 22 | 22 | 1 |
| 1 | 0 | 0 | 0 | 1 | 0 | 1 | 0 | 0 |
| 24 | 30 | 13 | 10 | 35 | 24 | 53 | 68 | 16 |
| 1 | 2 | 2 | 0 | 2 | 3 | 3 | 10 | 19 |
| 1 | 0 | 3 | 0 | 3 | 1 | 6 | 12 | 6 |
| 39 | 48 | 13 | 27 | 36 | 24 | 113 | 192 | 25 |
| 6 | 3 | 2 | 5 | 5 | 4 | 17 | 10 | 23 |
| 8 | 8 | 3 | 3 | 4 | 6 | 34 | 57 | 37 |
| 0 | 0 | 0 | 1 | 0 | 1 | 0 | 9 | 1 |
| 0 | 1 | 1 | 2 | 1 | 0 | 0 | 0 | 0 |
| 0 | 1 | 0 | 0 | 0 | 0 | 0 | 0 | 0 |
| 0 | 6 | 1 | 5 | 1 | 0 | 0 | 0 | 0 |
| 1 | 0 | 0 | 0 | 0 | 1 | 0 | 1 | 2 |
| 0 | 0 | 0 | 0 | 0 | 0 | 2 | 0 | 0 |
| 1 | 1 | 1 | 0 | 1 | 1 | 2 | 0 | 0 |
| 16 | 20 | 26 | 15 | 28 | 11 | 7 | 14 | 1 |
| 1 | 1 | 4 | 0 | 0 | 2 | 0 | 0 | 0 |
| 5 | 12 | 12 | 5 | 4 | 3 | 0 | 1 | 1 |
| 2 | 1 | 0 | 1 | 0 | 0 | 0 | 0 | 0 |
| 67 | 73 | 45 | 38 | 53 | 48 | 57 | 66 | 52 |
| 1 | 6 | 2 | 1 | 4 | 3 | 7 | 3 | 5 |
| 38 | 36 | 20 | 19 | 46 | 26 | 16 | 15 | 38 |
| 0 | 0 | 0 | 0 | 0 | 0 | 0 | 0 | 0 |
| 257 | 288 | 172 | 163 | 251 | 187 | 396 | 573 | 290 |
| 0 | 2 | 2 | 3 | 6 | 5 | 2 | 0 | 1 |

93SRLC14

| preservation | 3M M | 2M M | 1M G |
|---|---|---|---|
| Candeina nitida | 2 | 0 | 0 |
| Globigerina bulloides | 7 | 12 | 15 |
| Gna. falconensis | 0 | 0 | 0 |
| Gna. rubescens | 0 | 0 | 2 |
| Globigerinella aequilateralis | 13 | 12 | 46 |
| Gnl. calida | 1 | 3 | 15 |
| Gnl. digitata | 2 | 0 | 0 |
| Globigerinita glutinata | 27 | 23 | 56 |
| Globigerinoides conglobatus | 5 | 3 | 9 |
| Gds. elongatus | 1 | 0 | 1 |
| Gds. ruber | 37 | 51 | 150 |
| Gds. sacculifer | 3 | 5 | 17 |
| Gds. trilobus | 17 | 17 | 32 |
| Gds. tenellus | 0 | 0 | 0 |
| Globoquadrina conglomerata | 0 | 0 | 0 |
| Globorotalia bermudezi | 1 | 0 | 0 |
| Grt. crassaformis | 2 | 4 | 2 |
| Grt. hirsuta | 0 | 1 | 1 |
| Grt. inflata | 2 | 0 | 0 |
| Grt. scitula | 0 | 0 | 0 |
| Grt. menardii | 21 | 18 | 15 |
| Grt. truncatulinoides | 2 | 1 | 0 |
| Grt. tumida | 5 | 6 | 0 |
| Grt. ungulata | 1 | 0 | 0 |
| Neogloboquadrina dutertrei | 40 | 38 | 57 |
| Orbulina universa | 0 | 0 | 4 |
| Pulleniatina obliquiloculata | 13 | 23 | 21 |
| Sphaeroidinella dehiscens | 2 | 0 | 1 |
| PLANKTONI FORAM. TOTAL | 204 | 217 | 444 |
| BENTHIC FORAMINIFERA | 0 | 0 | 2 |

93SRLC20

| preservation | 10M G | 9M G | 8M G | 7M G | 6M G | 5M G | 4M G | 3M G | 2M G | 1M M |
|---|---|---|---|---|---|---|---|---|---|---|
| Candeina nitida | 0 | 0 | 0 | 0 | 2 | 0 | 0 | 0 | 0 | 0 |
| Globigerina bulloides | 17 | 16 | 13 | 8 | 9 | 12 | 9 | 7 | 19 | 15 |
| Gna. falconensis | 0 | 0 | 0 | 0 | 1 | 0 | 0 | 0 | 0 | 0 |
| Gna. rubescens | 0 | 1 | 2 | 0 | 2 | 0 | 0 | 1 | 0 | 0 |
| Globigerinella aequilateralis | 40 | 26 | 16 | 26 | 32 | 30 | 36 | 25 | 42 | 17 |
| Gnl. calida | 14 | 19 | 15 | 8 | 4 | 8 | 11 | 13 | 6 | 3 |
| Gnl. digitata | 0 | 0 | 0 | 3 | 0 | 0 | 0 | 0 | 0 | 3 |
| Globigerinita glutinata | 37 | 25 | 33 | 22 | 22 | 17 | 38 | 35 | 33 | 10 |
| Globigerinoides conglobatus | 1 | 3 | 2 | 3 | 6 | 6 | 9 | 5 | 7 | 13 |
| Gds. elongatus | 2 | 1 | 0 | 0 | 0 | 0 | 0 | 0 | 3 | 2 |
| Gds. ruber | 74 | 78 | 56 | 79 | 77 | 90 | 107 | 63 | 129 | 7 |
| Gds. sacculifer | 16 | 6 | 6 | 17 | 11 | 10 | 12 | 3 | 11 | 12 |
| Gds. trilobus | 18 | 7 | 22 | 18 | 12 | 19 | 16 | 12 | 28 | 26 |
| Gds. tenellus | 2 | 0 | 3 | 2 | 1 | 0 | 4 | 6 | 0 | 0 |
| Globoquadrina conglomerata | 0 | 0 | 0 | 0 | 0 | 0 | 0 | 0 | 0 | 0 |
| Globorotalia bermudezi | 0 | 0 | 0 | 0 | 1 | 0 | 0 | 0 | 0 | 0 |
| Grt. crassaformis | 0 | 0 | 0 | 0 | 0 | 0 | 0 | 0 | 0 | 0 |
| Grt. hirsuta | 1 | 1 | 0 | 1 | 0 | 0 | 0 | 2 | 0 | 1 |
| Grt. inflata | 0 | 0 | 0 | 0 | 0 | 0 | 0 | 0 | 0 | 0 |
| Grt. scitula | 1 | 2 | 0 | 1 | 0 | 0 | 0 | 0 | 0 | 0 |
| Grt. menardii | 11 | 2 | 7 | 7 | 4 | 0 | 0 | 0 | 0 | 0 |
| Grt. truncatulinoides | 0 | 0 | 0 | 0 | 0 | 0 | 0 | 0 | 0 | 0 |
| Grt. tumida | 0 | 0 | 0 | 0 | 0 | 0 | 0 | 0 | 0 | 9 |
| Grt. ungulata | 0 | 0 | 0 | 0 | 0 | 0 | 0 | 0 | 1 | 1 |
| Neogloboquadrina dutertrei | 36 | 33 | 34 | 18 | 23 | 18 | 21 | 18 | 34 | 60 |
| Orbulina universa | 2 | 5 | 2 | 1 | 1 | 2 | 3 | 0 | 0 | 3 |
| Pulleniatina obliquiloculata | 14 | 5 | 16 | 11 | 4 | 10 | 10 | 9 | 11 | 20 |
| Sphaeroidinella dehiscens | 0 | 0 | 0 | 0 | 0 | 0 | 0 | 0 | 0 | 1 |
| PLANKTONI FORAM. TOTAL | 286 | 230 | 227 | 225 | 212 | 222 | 276 | 199 | 324 | 203 |
| BENTHIC FORAMINIFERA | 0 | 1 | 0 | 1 | 1 | 1 | 1 | 2 | 0 | 1 |

Preservation

G:Good M:Moderate P:Poor VP:Very Poor

Table 4-2-1-2 Stratigraphic distribution of benthic foraminifera from cores (93SRLC06, 07, 14, 20)

| sample | 93-RLC06 | | | | | | | | | | | | |
|---|---|---|---|---|---|---|---|---|---|---|---|---|---|
| | 15M | 14M | 13M | 12M | 11M | 10M | 09M | 08M | 07M | 05M | 04M | 03M | 01M |
| **Agglutinated foraminifera** | | | | | | | | | | | | | |
| *Rhabdammina abyssorum Sars* | | | | + | | | | + | + | | | | + |
| *Cribrostomoides subglobosum (Sars)* | | | | + | | + | | | | | | | |
| *Eggerella bradyi (Cushman)* | | | + | + | | | | | | | | | |
| *Karreriella bradyi* | + | | + | | | + | | + | + | | | | |
| *Siphotextularia sp.* | | | | | | | | | | | | + | |
| **Calcareous foraminifera** | | | | | | | | | | | | | |
| *Pyrgo depressa (d' Orbigny)* | | | | | | + | | | | | | | |
| *Pyrgo murrhina (Schwager)* | | | | + | | | | | | | | | |
| *Miliolidae gen. et sp. indet.* | | | | | + | | | | | | | | |
| *Lagena hispidula Cushman* | | | | | | | | + | | | | | |
| *Pyrulina angusta (Egger)* | | | + | | | | | | | | | | |
| *Pyrulina fusiformis (Roemer)* | | | | + | | | | | | | | | |
| *Polymorphinidae gen. et sp. indet* | | | | + | | | | | | | | | |
| *Fissurina alveolata semisculpta Parr* | | | | + | | + | | + | | | | | |
| *Fissurina flintiana (Cushman)* | | | + | + | | | | | | | | | |
| *Fissurina radiata Seguenza* | + | | + | | | + | | | | | | | |
| *Fissurina submarginata (Boomgart)* | | | + | | | | | | | | | | |
| *Fissurina spp.* | | | | + | | + | | + | | | | + | |
| *Evolvocassidulina sp.* | | | | + | | | | | | | | | |
| *Favocassidulina favus (Brady)* | | | | | | | | + | | | | | |
| *Globocassidulina murrhyna (Schwager)* | | | + | + | | | | | | | | | |
| *Globocassidulina subglobosa (Brady)* | + | + | + | + | | | + | + | + | | | | |
| *Ehrenbergina carinata Eade* | | | | + | | | | | | | | | |
| *Uvigerina peregrina Cushman* | | | + | | | | | | | | | | |
| *Sphaeroidina bulloides d' Orbigny* | | | + | + | | | | | | | | | |
| *Cibicidoides mundulus (Brady, Parker & Jones)* | | | | | | | + | | | | | | |
| *Epistominella exigua (Brady)* | | | + | + | | + | | | | | | | |
| *Laticarinina pauperata (Parker & Jones)* | | | | | | | | + | | | | | |
| *Planulina sp.* | | | | | | | | | | | | | |
| *Cibicides cf.refulgens Montfort* | | | + | | | | | + | | | | | |
| *Fontbotina wuellerstorfi (Schwager)* | | | + | + | + | | | | | | | | |
| *Nuttallides umboniter (Cushman)* | + | | + | + | | + | + | + | + | | | | + |
| *Astrononion umbilicatulum (Uchio)* | | | | | | | | | + | | + | | |
| *Melonis barleeasum (Williamson)* | + | | + | | + | | + | + | | | | + | |
| *Melonis sphaeroides Voloshinova* | | | + | + | | + | + | + | | | + | + | |
| *Pullenia bulloides (d' Orbigny)* | | | + | + | | | + | | + | | | | |
| *Pullenia quinqueloba (Reuss)* | | | + | + | | | + | | | | | | |
| *Pulleniella asymmetrica Ujiie* | + | | + | + | + | | | | + | + | | | |
| *Oridorsalis tener (Brady)* | | | + | + | | | | | | | + | | |
| *Anomalinoides globulosus (Chapman & Parr)* | | | | + | | | + | | | | | | + |
| *Gyroidinoides neosoldanii* | + | | + | + | | | | + | + | | | | |
| *Gyroidinoides soldanii (d' Orbigny)* | | | + | + | | | | | | | | | |
| *Gyroidina sp. A* | + | + | | + | | | | + | | + | | | |

| sample | 93-RLC07 | | | | | | | 93-RLC14 | 93-RLC20 | | | | | |
|---|---|---|---|---|---|---|---|---|---|---|---|---|---|---|
| | 08M | 07M | 06M | 05M | 04M | 03M | 01M | 01M | 09M | 07M | 06M | 05M | 04M | 03M | 01M |
| **Agglutinated foraminifera** | | | | | | | | | | | | | | | |
| *Rhabdammina abyssorum Sars* | | | | | | | | | | | | | | | |
| *Cribrostomoides subglobosum (Sars)* | | | | | | | | | | | | | + | + | |
| *Eggerella bradyi (Cushman)* | | | | | + | | | | | | | | | | |
| *Karreriella bradyi* | | + | | | + | | | | | | | | | | |
| *Siphotextularia sp.* | | | | | | | | | | | | | | | |
| **Calcareous foraminifera** | | | | | | | | | | | | | | | |
| *Pyrgo depressa (d' Orbigny)* | | | | | | | | + | | | | | | | |
| *Pyrgo murrhina (Schwager)* | | | | | | | | | | | | | | | |
| *Miliolidae gen. et sp. indet.* | | | | | | | | | | | | | | | |
| *Lagena hispidula Cushman* | | | | | | | | | | | | | | | |
| *Pyrulina angusta (Egger)* | | | | | | | | | | | | | | | |
| *Pyrulina fusiformis (Roemer)* | | | | | | | | | | | | | | | |
| *Polymorphinidae gen. et sp. indet* | | | | | | | | | | | | | | | |
| *Fissurina alveolata semisculpta Parr* | | | | | | | | | | | | | | | |
| *Fissurina flintiana (Cushman)* | | | | | | | | | | | | | | | |
| *Fissurina radiata Seguenza* | | | | | + | | | | | | | | | | |
| *Fissurina submarginata (Boomgart)* | | | | | | | | | | | | | | | |
| *Fissurina spp.* | | | | | | | | | | | | | | | |
| *Evolvocassidulina sp.* | | | | | | | | | | | | | | | |
| *Favocassidulina favus (Brady)* | | + | | | | | | | | | | | | | |
| *Globocassidulina murrhyna (Schwager)* | | | | | | | | | | | | | | | + |
| *Globocassidulina subglobosa (Brady)* | | | | | | | | | | | | | | | |
| *Ehrenbergina carinata Eade* | | | | | | | | | | | | | | | |
| *Uvigerina peregrina Cushman* | | | | | | | | | | | | | | | |
| *Sphaeroidina bulloides d' Orbigny* | | | | + | | + | | | | | | | | | |
| *Cibicidoides mundulus (Brady, Parker & Jones)* | | | | | | | | | | | | | | | |
| *Epistominella exigua (Brady)* | | | + | + | | | | | | | | | | | |
| *Laticarinina pauperata (Perker & Jones)* | | | | | | | | | | | | | | | |
| *Planulina sp.* | | | | | | | | | | | | + | | | |
| *Cibicides cf.refulgens Montfort* | | | | | | | | | | | | | | | |
| *Fontbotina wuellerstorfi (Schwager)* | | | | | | | | | | | | | | | |
| *Nuttallides umboniter (Cushman)* | | | | + | | | | | | | | | | | |
| *Astrononion umbilicatulum (Uchio)* | | | | | + | | | | | | | | | + | |
| *Melonis barleeasum (Williamson)* | + | | | | | + | | + | | | + | + | | | |
| *Melonis sphaeroides Voloshinova* | | | + | | + | | | | | | | | | | |
| *Pullenia bulloides (d' Orbigny)* | + | | | + | | | | | | | | | | | |
| *Pullenia quinqueloba (Reuss)* | | | | | + | + | | | + | | | | | | |
| *Pulleniella asymmetrica Ujiie* | | | | | | | | | | | | | | | |
| *Oridorsalis tener (Brady)* | | | + | | | | | | | | | | | | |
| *Anomalinoides globulosus (Chapman & Parr)* | | | | | | | | | | | | | | | |
| *Gyroidinoides neosoldanii* | | | | | | | | | | | | | | | |
| *Gyroidinoides soldanii (d' Orbigny)* | | | | | | | | | | | | | | | |
| *Gyroidina sp. A* | | | | + | | | | | | | | | | | |

N23 zone (between 0 and 0.3 Ma). This fact is also substantiated by the facts that the spiral direction of the *Pulleniatina* genus in the samples is entirely indicating clockwise and occurrence of *Globoquadrina conglomerata* occurs. *Globigerinoides ruber* with pink shells (hereinafter referred to as "*Globigerinoides ruber* (pink)" occur in the samples -7M and -3M. Thompson et al. (1979) place the horizon in India-Pacific region on which this *Globigerinoides ruber* (pink) ceased to exist at 0.12 Ma, so the upper layers above the sample -3M, on which *Gds. ruber* (pink) ceased to exist in this core, is considered as dating younger than 0.12 Ma.

The samples of the lower half of this core (-8M, -10M, -12M and -13M) are relatively abundant in benthic foraminiferas, which amounts to 20 individuals to 60 individuals, but many of them are ill-preserved. It may well be that they were resedimented. Except these, the composition of fossil communities are the same from top to bottom of this core. All of them are constructed by the species characterizing the area from the mid-bathyal zone to the abyssal zone. The species occurring in the shoal shallower than the upper bathyal zone are also identified, but very few. All of them are ill-preserved individuals and considered as resedimented.

- 93SRLC07

The detection results of planktonic foraminiferous fossils from this core's 9 samples are shown in Table 4-2-1-1, and the detection results of benthic foraminiferous fossils are shown in Table 4-2-1-2.

The planktonic foraminiferous fossils obtained from this core is well-preserved. This core is, in the aggregate, considered as indicating the N23 zone (between 0 Ma and 0.3 Ma) from the facts that *Globorotalia truncatulinoides* and *Globigerinella calida* occur in the sample taken out from the lowest part (-9M), that the spiral direction of the *Pulleniatina* genus in every sample is indicating clockwise and that *Globoquadrina conglomerata* occur in this core. *Globigerina rubescens* with pink shells (hereinafter referred as "*Globigerina rubescens* (pink)" pointed out by Saito et al. (1981) as existing from the latter period of the Pleistocene Epoch to the Recent Epoch occur in the samples -8M and -4M. These facts can be considered as substantiating the above-mentioned age presumption. *Globigerinoides ruber* (pink), however, is

not identified from this core's samples, so it is difficult to discuss this matter further.

The benthic foraminiferous fossils detected from the samples of this core is entirely composed of the species characterizing the area from the mid-bathyal zone to the abyssal zone. The species occurring in the shoal shallower than the upper bathyal zone are also identified, but very few. All of them are ill-preserved individuals and considered as resedimented. As the occurrence number of the benthic foraminiferous fossils is few, it is difficult to discuss the variation between the upper part and lower part.

- 93SRLC14

The detection results of planktonic foraminiferous fossils from this core's 3 samples are shown in Table 4-2-1-1, and the detection results of benthic foraminiferous fossils are shown in Table 4-2-1-2.

The planktonic foraminiferous fossils obtained from this core is, in the aggregate, relatively well-preserved. As in the case of 93SRLC07, this core is, in the aggregate, considered as indicating the N23 zone (between 0 Ma and 0.3 Ma) from the facts that *Globorotalia truncatulinoides* and *Globigerinella calida* occur in the sample taken out from the lowest part (-3M), that the spiral direction of the *Pulleniatina* genus in every sample is indicating clockwise and that *Globigerina rubescens* (pink) occur in the sample -1M. *Globigerinoids ruber* (pink), however, is not identified from this core's samples, so it is difficult to discuss this matter further.

The benthic foraminiferous fossils detected from the samples of this core is entirely composed of the species characterizing the area from the mid-bathyal zone to the abyssal zone. The species occurring in the shoal shallower than the upper bathyal zone are also identified, but very few. All of them are ill-preserved individuals and considered to be resedimented. As the occurrence number of the benthic foraminiferous fossils is few, it is difficult to discuss the variation between the upper part and lower part.

- 93SRLC20

The detection results of planktonic foraminiferous fossils from this core's 10 samples are shown in Table 4-2-1-1, and the detection results of benthic

foraminiferous fossils are shown in Table 4-2-1-2.

The planktonic foraminiferous fossils obtained from this core is, in the aggregate, very well-preserved. This core is, in the aggregate, considered as indicating the N23 zone (between 0 Ma and 0.3 Ma) from the facts that *Globorotalia truncatulinoides* and *Globigerinella calida* occur in the sample taken out from the lowest part (-10M), that the spiral direction of the *Pulleniatina* genus in every sample is indicating clockwise and that *Globigerina rubescens* (pink) occur in the entire core. *Globigerinoides ruber* (pink), occur in the samples -4M and -3M of this core, so the upper layers above the upper bound sample -3M is considered as dating younger than 0.12 Ma.

The benthic foraminiferous fossils detected from the samples of this core is entirely composed of the species characterizing the area from the mid-bathyal zone to the abyssal zone. The species occurring in the shoal shallower than the upper bathyal zone are also identified, but very few. All of them are ill-preserved individuals and considered as resedimented. As the occurrence number of the benthic foraminiferous fossils is few, it is difficult to discuss the variation between the upper part and lower part.

Here we will discuss the community composition of the planktonic foraminiferous fossils. The ratio of community composition classified by genus on each sample is shown in Fig. 4-2-1-5.

28 species of 11 genera of planktonic foraminiferous fossils are identified from 37 samples. The most of the genera of these planktonic foraminiferous fossils are *Globigerinoides, Globigerinella, Globigerinita, Globorotalia, Pulleniatina* and *Neogloboquadrina*. These six genera account for 90% of all individuals occurred. *Gds. ruber* and *Gds. sacculifer* are the predominant species as the *Globigerinoides* genus, *Grt. menardii* and *Grt. tumida* are the predominant species as the *Globorotalia* genus, and *Gnl. aequilateralis* is the predominant species as the *Globigerinella* genus. The preservation state of the planktonic foraminiferous fossils with the exception of 93SRLC20 is not always good. They are affected by dissolution. According to the study on the effect of solution to thanatocoenoses of planktonic foraminiferas with calcium carbonate shells (Berger et al. 1970 and so on), generally, *Globorotalia* and *Pulleniatina* genera are resistant to

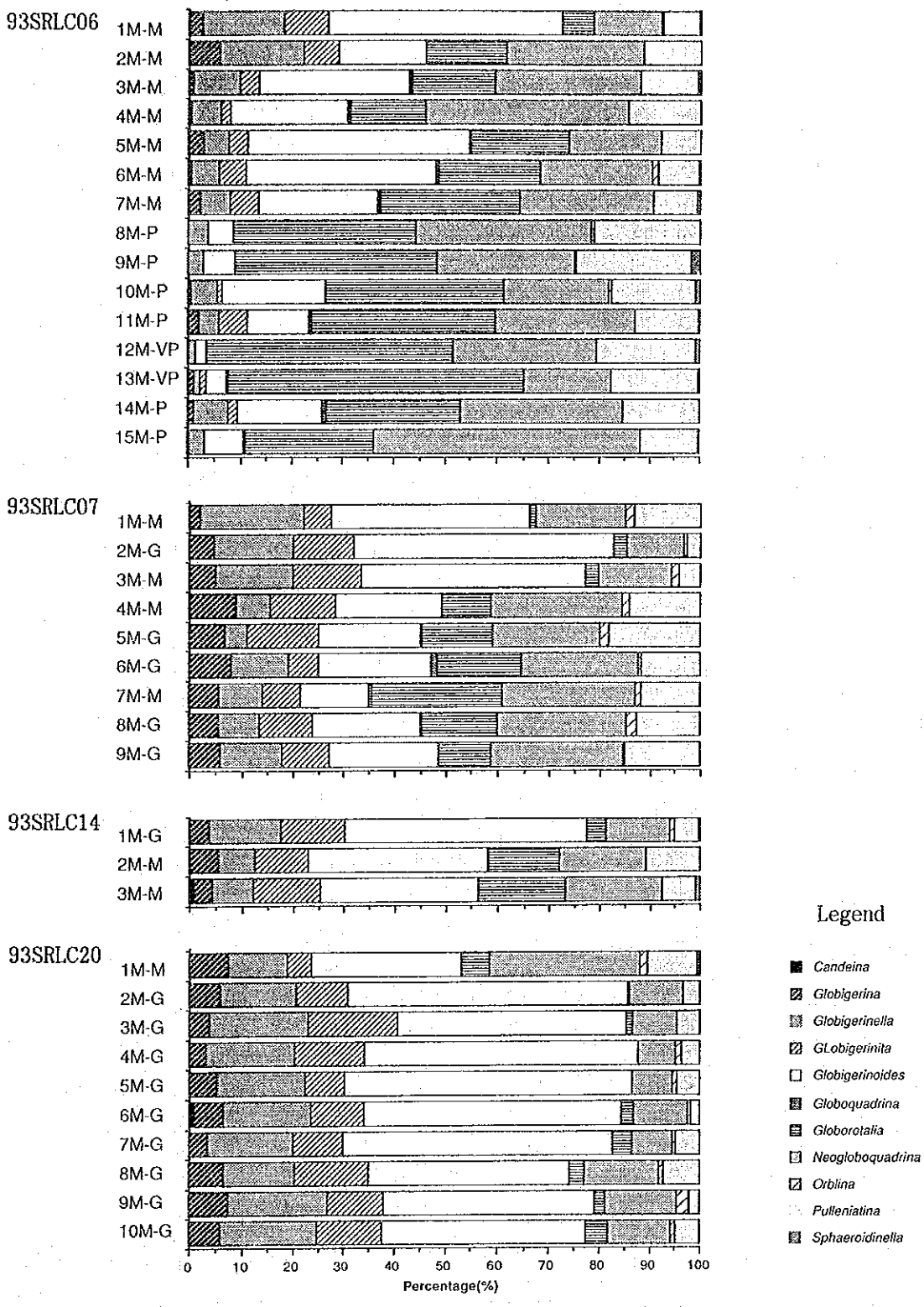


Figure 4-2-1-5 Percent abundance of each genus of planktonic foraminifera from cores (93SRLC06, 07, 14, 20)

dissolution, but *Globigerinoides*, *Globigerinella* and *Globigerina* genera are easily affected by dissolution. It is, therefore, known that juvenile community composition will alter, because dissolution has a different effect on a different indigenous character of species and the dissolution functions selectively on species. Such dissolution is considered as deeply correlating with sedimentary depth, producing volume and bottom current.

Planktonic foraminiferous fossils in the lower half of the core 93SRLC06 are ill-preserved and the percentage of community species has been changed by dissolution as stated above. For instance, the frequency of occurrence of the *Globorotalia* genus and *Pulleniatina* genus - they are resistant to dissolution - in the lower half of the core is relatively greater in number when compared with the upper half. On the other hand, the frequency of occurrence of the *Globigerinoides* genus, *Globigerinella* genus and *Globigerina* genus - they are easily affected by dissolution - in the lower half of the core is relatively fewer in number when compared with the upper half. This means that the influence of dissolution is great in this core. Among the four cores, the occurrence frequency of the *Globigerinoides* genus, *Globigerinella* genus and *Globigerina* genus is high in the core 93SRLC20, whose planktonic foraminiferous fossils are preserved in the best condition. So, we can presume that these foraminiferous fossils are least affected by dissolution. The preservation condition of cores 93SRLC14 and 93SRLC07 are in-between those two cores.

Now we will estimate the sedimentary environment. Planktonic foraminiferous fossil groups among the samples are mainly composed of the species abundant in low-latitudes such as *Globigerinoides ruber, Gds. sacculifer, Globigerinella aequilateralis, Globorotalia menardii, Grt. tumida, Neogloboquadrina dutertrei* and *Pulleniatina obliquiloculata*. And the groups also include the species abundant in horse latitudes such as *Globorotalia truncatulinoides, G. inflata, Globigerina bulloides* and so on. From these, the planktonic foraminiferous fossils indentified in these samples are considered as the groups indicating the geographic divisions from the tropical zone to the subtropical zone. According to Be (1977), *Globigerinoides ruber*, which is abundant in the samples not so affected by dissolution, occurs roughly between 45° N and 45° S, but this species is, if anything, abundant in the geographic division of subtropical zone.

Benthic foraminiferous fossils identified in the samples are composed of the species characterizing the area from the mid-bathyal zone to the abyssal zone.

Now we will discuss the rate of sedimentation. All cores under this analysis belong to the N23 zone, and because the range of age is narrow, there is little index datum as appearance or disappearance of planktonic foraminiferas. There are only the lower limit for the occurrence of *Globigerinella calida* and the disappearing horizon of *Globigerinoides ruber* (pink) that can be used for setting up index datum, so it is difficult to presume a strict rate of sedimentation.

Supposing that the horizon on which *Globigerinoides ruber* (pink) disappears as the sample -3M of the core 93SRLC06, then the rate of sedimentation at around the surface (-1M and -2M) is presumed to be 2.5 mm/ka and supposing that the lower limit horizon for the occurrence of *Gnl. calida* as the sample -14M, then the rate of sedimentation at lower than the sample -3M is presumed to be about 3.7 mm/ka. The planktonic foraminiferous fossils in the lower half of this core are badly preserved, especially, this tendency is conspicuous in the samples -12M and -13M. In these two samples, the benthic foraminiferous fossils have a majority in all foraminiferous fossils. Generally, benthic foraminiferous fossils are more resistant to dissolution than planktonic foraminiferous fossils, so this percentage in deep-sea sediments can be a relative index of dissolution. We, therefore, can presume that the rate of sedimentation at the samples lower than -3M of this core was not fixed, and that the samples -12M and -13M were considerably affected by the solution, because of slower rate of sedimentation. In this case, the lower part shows a higher rate of sedimentation than the surface part, this may be attributed to the selection of the sample -14M as the lower limit of the occurrence of *Gnl. calida.*

Supposing that the horizon on which *Globigerinoides ruber* (pink) disappears as the sample -3M of the core 93SRLC20, then the rate of sedimentation at around the surface (-1M and -2M) is presumed to be 2.5 mm/ka and supposing that the lower limit horizon for the occurrence of *Gnl. calida* as the sample of the lowest part (-10M), then the rate of sedimentation is presumed to be about 2.3 mm/ka.

The occurrence of *Glogigerinoides ruber* (pink) is not identified in the cores 93SRLC07 and 93SRLC14. Furthermore, *Gnl. calida* occurs in the sample

of the lowest part of the core. It is difficult to estimate the rate of sedimentation as we cannot identify the index datum of these two cores.

<Mechanical analysis of Seafloor sediments>

With the objective of estimating the sedimentary environment, vertical and continuous sampling was conducted at four points (i.e. 93SRLC06, 93SRLC07, 93SRLC14 and 93SRLC20) among the sampling points for the regional survey. And the grain size distribution of the constitutive grains was measured. Samples were collected at intervals of 20 cm counting from the upper layer (submarine surface). The number of samples are 15 samples from 93SRLC06 (-1S to -15S), 9 samples from 93SRLC07 (-1S to -9S), 3 samples from 93SRLC14 (-1S to -3S) and 10 samples from 93SRLC20 (-1S to -10S), totaling 37 samples.

Measuring items are the density (only the surface part) and grain size distribution.

The density of the samples was measured by the "Method of testing the density of soil grains" (JSF T 111-1990) of the Standard of Soil Engineering Institute.

Samples taken from the surface part (10cm deep) of the cores were measured. The results are used in the measurement of grain sizes in each core. The samples were dried at 110℃ by an oven and put in Gay-Lussac's Pycnometers for more than 12 hours with water. Then, they were boiled quietly for more than 10 minutes to remove air bubbles. After that the samples were weighed and the density was calculated.

Grain sizes were measured by the "Method of test grain sizes of soil" (JSF T 131-1990) of the Standard of Soil Engineering Institute. The mass of the sample was measured. Then the sample were washed with water on a 75 $\mu$m sieve. The remaining substances on the sieve were dried by an oven before they were analyzed by the seive analysis methods. Soil grains under 75 $\mu$m, which had passed the 75 $\mu$m sieve, were measured by the precipitation method.

The measuring results of the density are as follows:

93SRLC06-01S : 2.741 g/cm$^3$

93SRLC07-01S : 2.686 g/cm$^3$

93SRLC14-01S : 2.735 g/cm$^3$

93SRLC20-01S : 2.778 g/cm$^3$

Grain size distribution was measured by the sieve method and precipitation method, and a cumulative curve of grain sizes was obtained from the results of these

methods. In order to obtain the grain size distribution of the finer grains, cumulative frequency distribution was plotted on a logarithmic probability paper to draw up a cumulative frequency distribution curve.

Coefficients of grain sizes were calculated by the method of the Society for the study of Clastic Deposits (1983). Each percentile grain size required for calculation was read by the illustration method. Its results are shown in Fig. 4-2-1-6. These results were also converted into $\phi$ scale and median diameters, mean diameters and sorting indexes were obtained by the formula of Folk & Ward (1957). These results are shown in Table 4-2-1-3. The median diameters and mean diameters are converted from the $\phi$ scale into $\mu$m unit in the said Table. This method of calculating the sorting indexes, however, is mainly used for the grain size analysis of sandstone, are not generally applied for extremely fine-grained seafloor sediments like the present samples.

The formula of Folk & Ward (1957) for obtaining the coefficient of each grain size and the evaluation of sorting indexes are shown below:

Mediam diameter $Md\phi = \phi_{50}$

Mean diameter $Mz = (\phi_{16} + \phi_{50} + \phi_{84})/3$

Sorting index $\sigma_1 = (\phi_{84} - \phi_{16})/4 + (\phi_{95} - \phi_5)/6.6$

| | |
|---|---|
| <0.35 | : very well sorted |
| 0.35 ~ 0.50 | : well sorted |
| 0.50 ~ 0.71 | : moderately well sorted |
| 0.71 ~ 1.00 | : moderately sorted |
| 1.00 ~ 2.00 | : poorly sorted |
| 2.00 ~ 4.00 | : very poorly sorted |
| >4.00 | : extremely poorly sorted |

The characteristics of grain size distribution classified by the sampling point are as follows. In the case of extremely fine-grained samples, the width of grain size's $\phi$ values becomes very wide when compared with the width of sandstone, so every sample's sorting index becomes large (bad). As the calculation method of Folk & Ward (1957) is mainly used to evaluate the grain size of sandstone. So it is questionable whether it can be applied to such fine-grained samples like the present case.

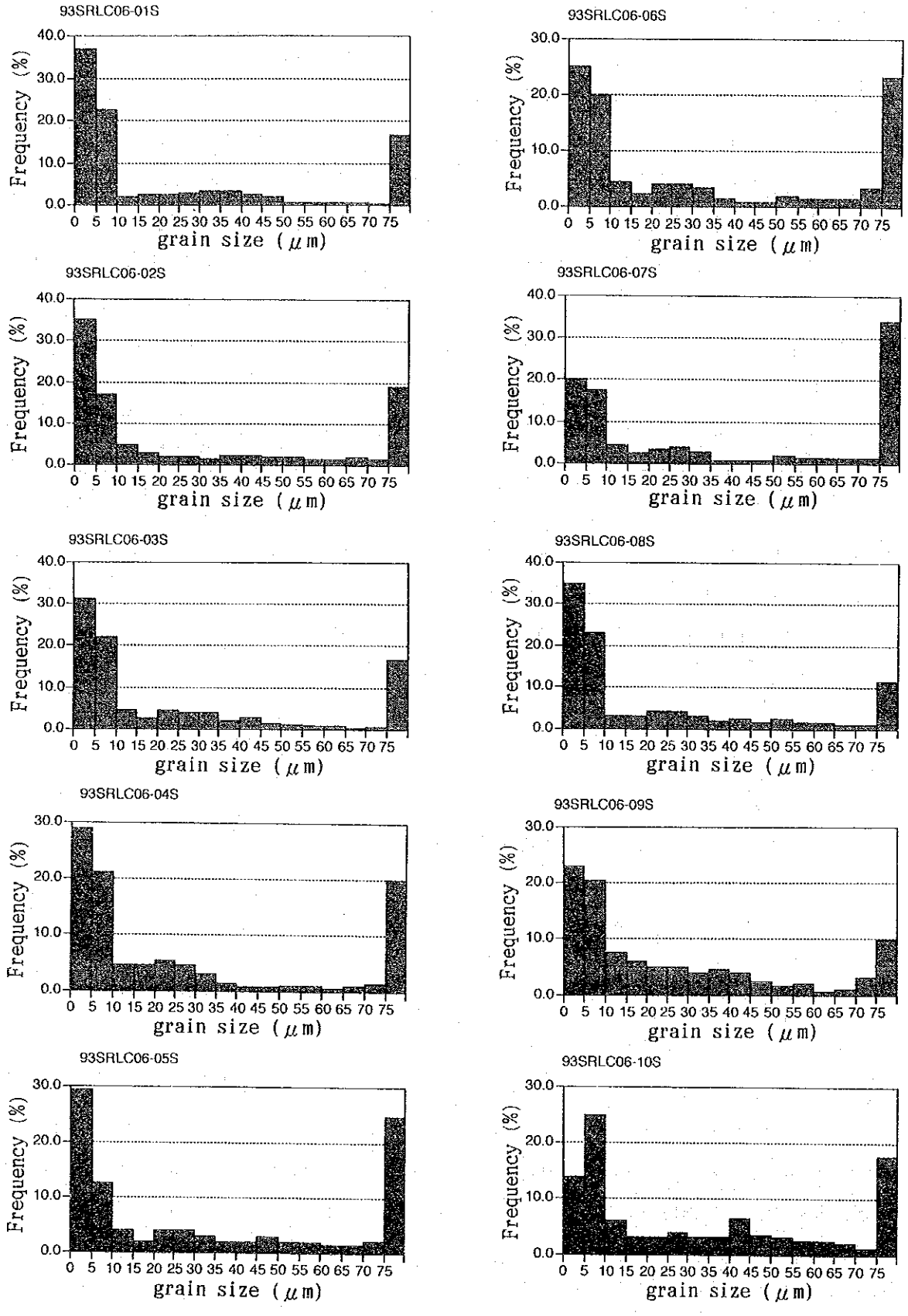


Figure 4-2-1-6 Histogram of grain size (1)

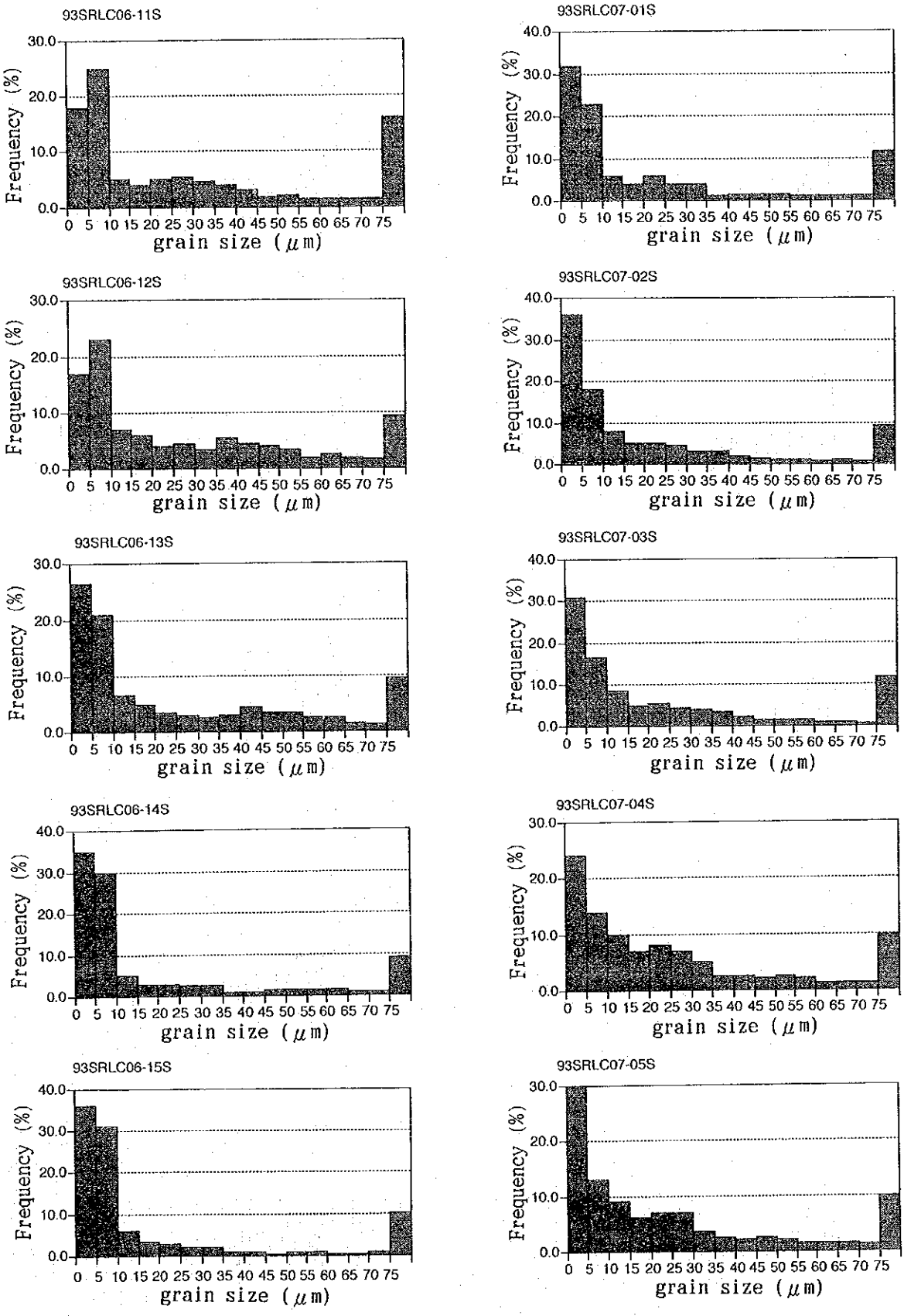


Figure 4-2-1-6 Histogram of grain size (2)

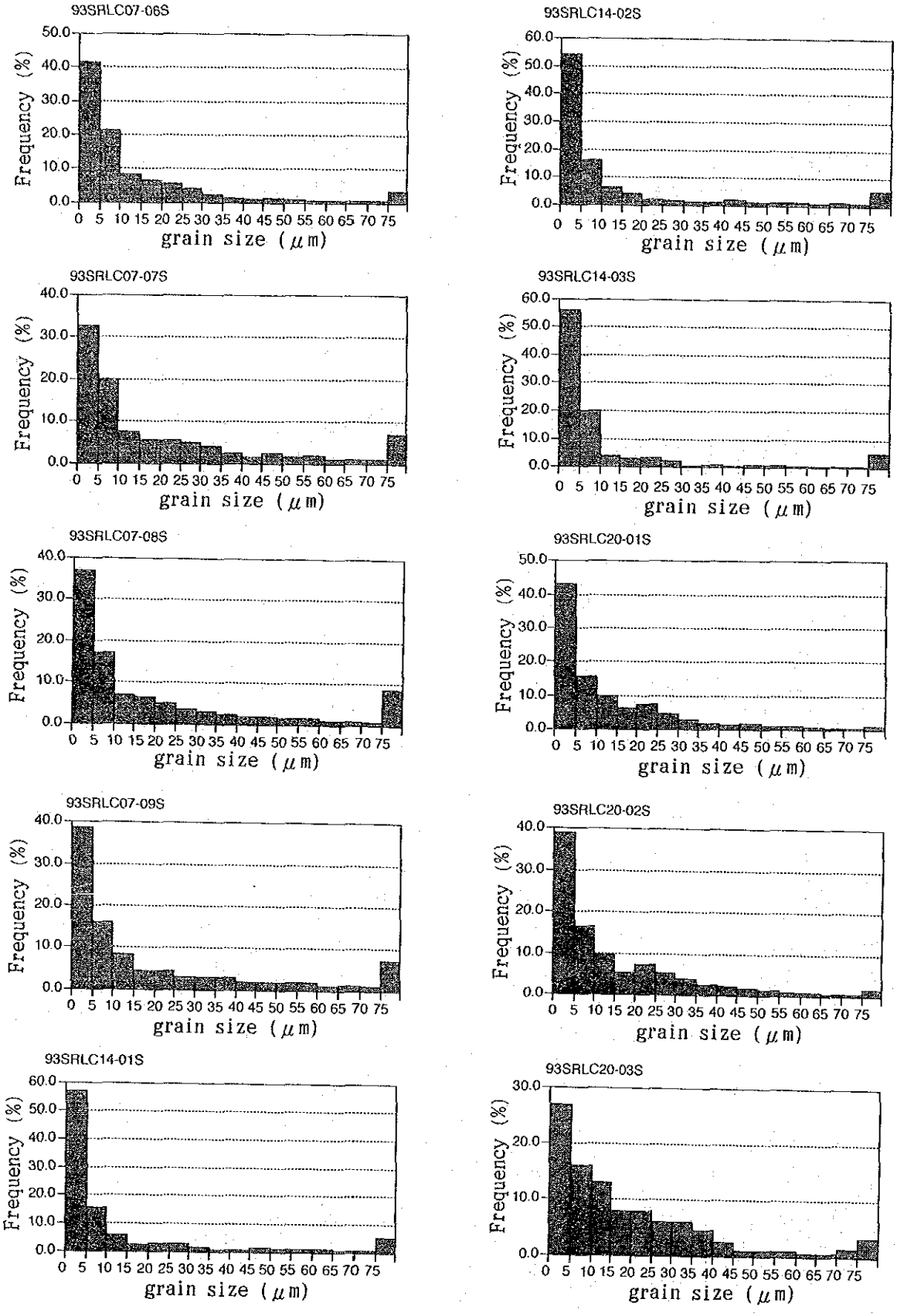


Figure 4-2-1-6 Histogram of grain size (3)

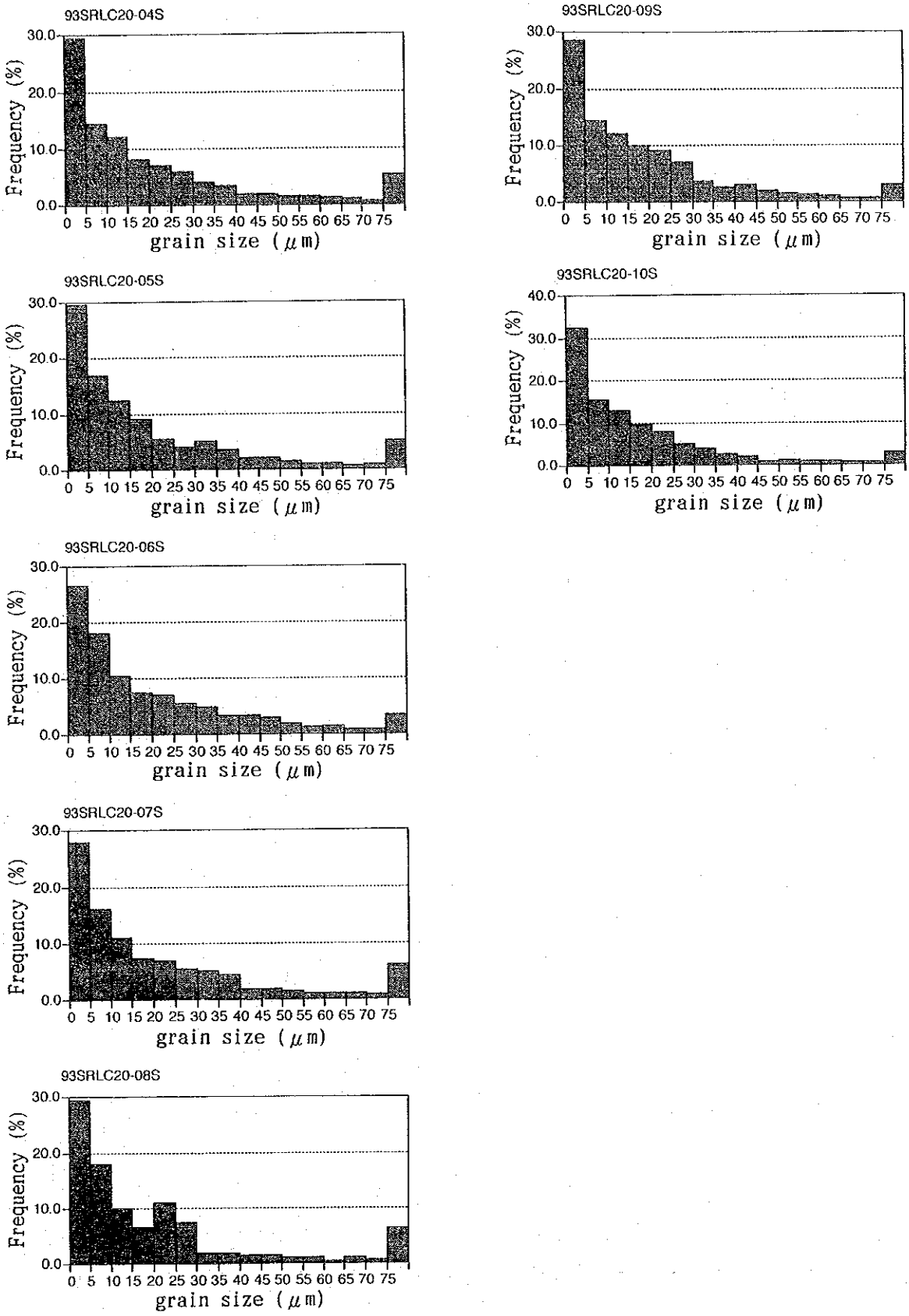


Figure 4-2-1-6 Histogram of grain size (4)

Table 4-2-1-3 Results of mechanical analysis of sediments

| Sample No. | median diameter | mean diameter | sorting coefficient | 75μm≦Frequency |
|---|---|---|---|---|
| 93SRLC06-01S | 6.0 | 11.5 | 2.45 | 16.6 |
| 93SRLC06-02S | 8.6 | 13.1 | 2.53 | 19 |
| 93SRLC06-03S | 7.5 | 12.9 | 2.28 | 16.8 |
| 93SRLC06-04S | 10.0 | 15.3 | 2.29 | 20.1 |
| 93SRLC06-05S | 23.0 | 19.1 | 2.50 | 24.8 |
| 93SRLC06-06S | 15.5 | 18.5 | 2.54 | 23.1 |
| 93SRLC06-07S | 27.5 | 24.4 | 2.26 | 34 |
| 93SRLC06-08S | 6.6 | 11.0 | 2.16 | 11.6 |
| 93SRLC06-09S | 14.0 | 14.7 | 2.01 | 9.9 |
| 93SRLC06-10S | 23.0 | 21.5 | 1.94 | 17.7 |
| 93SRLC06-11S | 17.0 | 18.2 | 2.00 | 16.1 |
| 93SRLC06-12S | 17.5 | 17.1 | 1.82 | 9.3 |
| 93SRLC06-13S | 12.0 | 13.7 | 2.09 | 9.6 |
| 93SRLC06-14S | 6.0 | 10.1 | 2.10 | 9 |
| 93SRLC06-15S | 6.2 | 9.3 | 1.94 | 10.2 |
| 93SRLC07-01S | 8.0 | 11.1 | 2.09 | 11.5 |
| 93SRLC07-02S | 8.0 | 9.5 | 2.09 | 9.2 |
| 93SRLC07-03S | 11.0 | 10.4 | 2.49 | 11.8 |
| 93SRLC07-04S | 16.5 | 14.0 | 2.04 | 9.8 |
| 93SRLC07-05S | 13.5 | 11.9 | 2.17 | 9.8 |
| 93SRLC07-06S | 6.2 | 7.0 | 1.82 | 3.4 |
| 93SRLC07-07S | 8.8 | 8.3 | 2.76 | 7 |
| 93SRLC07-08S | 8.4 | 9.2 | 2.17 | 8.7 |
| 93SRLC07-09S | 8.2 | 8.8 | 2.23 | 7.4 |
| 93SRLC14-01S | 3.5 | 5.0 | 2.05 | 5.3 |
| 93SRLC14-02S | 4.5 | 5.7 | 2.19 | 5.4 |
| 93SRLC14-03S | 4.4 | 5.3 | 1.92 | 5.1 |
| 93SRLC20-01S | 7.0 | 6.4 | 1.99 | 1.2 |
| 93SRLC20-02S | 8.2 | 7.8 | 1.89 | 1.7 |
| 93SRLC20-03S | 12.0 | 10.6 | 1.78 | 3.4 |
| 93SRLC20-04S | 12.3 | 10.8 | 1.89 | 5.4 |
| 93SRLC20-05S | 11.5 | 10.2 | 1.90 | 5 |
| 93SRLC20-06S | 13.0 | 11.6 | 1.84 | 3.4 |
| 93SRLC20-07S | 12.0 | 10.2 | 2.07 | 6.1 |
| 93SRLC20-08S | 11.0 | 9.6 | 1.91 | 6.3 |
| 93SRLC20-09S | 12.5 | 10.0 | 1.92 | 2.9 |
| 93SRLC20-10S | 11.0 | 8.8 | 1.89 | 2.9 |

• 93SRLC06

The median diameters of the samples of this core are between 6.0 μm and 27.5 μm and their mean diameters are between 9.2 μm and 24.4 μm. Although the values of each sample vary widely but every sample's grain sizes are within the range from fine-grained silts to medium-grained silts. Their sorting indexes are from 1.82 to 2.54, which are relatively worse than the samples of other cores. Every sample has a sharp peak of smaller than 10 μm on the histogram of the grain size. Some of them show multi-peak frequency distribution of having more than two of very small peaks. All of the samples have more than 10% of coarse grains larger than 75 μm. The frequencies of coarse grains larger than 75 μm are between 17% and 19% at -01S to -03S, between 20% and 34% at -04S to -07S, about 10% at -08S to -09S, between 16% and 18% at -10S to -11S and between 9% and 10% at -12S to -15S. About the same frequencies of coarse grains continue at intervals between 20 cm and 40 cm. From which we can presume that the thickness of one sedimentary unit is between 20 cm and 40 cm, and has changed at least five times.

• 93SRLC07

The median diameters of the samples of this core are between 6.2 μm and 16.5 μm and their mean diameters are between 7.0 μm and 14.0 μm. Although the values of each sample vary widely but every sample's grain size are within the range from micro-grained silts to fine-grained silts. Their sorting indexes are from 1.82 to 2.76.

Many samples have a sharp peak of smaller than 10 μm on the histogram. Some of them show multi-peak frequency destribution of having one or two small peaks. The sizes of these small peaks correspond to the values of the median and mean diameters. The frequencies of coarse grains larger than 75 μm are about 10% at -01S to -05S, which values are rather high, and less than 10% at -06S to -09S, which are rather low. These phenomena also appear in the differences of mean diameters. Especially in the cases of -04S and -05S, their mean diameters are larger than those of other samples because there are relatively larger peaks between the 10 μm and 40 μm. From these variations in the patterns of frequency distribution, we can presume that the facies of these seafloor sediments have changed at least three times.

· 93SRLC14

The median diameters of the samples of this core are between 3.5 μm and 4.5 μm and their mean diameters are between 5.0 μm and 5.7 μm. The values of each sample vary hardly and show the grain sizes of micro-grained silts. The sorting indexes are between 1.92 and 2.19. The patterns of the samples resemble each other. Grains of smaller than 5 μm account for more than 50% of all and their mean diameter is about 5 μm, which is rather fine. Very small peaks are also identified between 15 μm and 35 μm, and between 40 μm and 60 μm. Coarse grains of larger than 75 μm account for about 5% in every sample, which is relatively low. From these, we can presume that the facies of these seafloor sediments have hardly changed and constitute nearly the same horizons.

· 93SRLC20

The median diameters of the samples of this core are between 7.0 μm and 13.0 μm and their mean diameters are between 6.4 μm and 11.6 μm. Although the values of each sample vary widely but sample's grain sizes are within the range between micro-grained silts and fine-grained silts. The sorting indexes are from 1.84 to 2.07. Every sample has a sharp peak of smaller than 5 μm on the histogram. Samples with one or two weak peaks are also indentified frequently. In the aggregate, coarse grains of larger than 75 μm are few. The frequency distribution patterns of -01S and -02S resemble each other and have many grains of smaller than 5 μm, and the mean diameters are relatively small. Except these two, the mean diameters and median diameters of the samples are almost the same and their frequency distribution patterns also resemble each other. Only -08S has conspicuous peaks between the sizes of 20 μm and 25 μm, which differs from other patterns. So we can see that the facies of this core have changed at least twice.

2) Rocks

As the sampling target of the regional survey was muddy sediments, so the rock samples obtained through this survey were extremely scarce. Furthermore, as the corer's power to penetrate rock masses was not so strong, so the collected samples were fragmented rocks with diameters of several cm at the most.

Among the 24 planned sampling points for the regional survey, the tips of the corer's bit were deformed at 5 points (i.e. 93SRGC01, 93SRGC11, 93SRLC14, 93SRGC22 and

93SRGC25). Rocks collected from two points (93SRGC01 and 93SRGC11) among these 5 points and another point at 93SRGC18, totaling three points. These rocks are basalt with plagioclase phenocryst when examined with the naked eye, and olivine phenocryst is also observed in a part of these rocks. A few black hyaline parts were also collected.

We conducted the observation of thin sections and whole rock analysis for the samples collected. The results are as follows.

Some rocks were also collected by the chain buckets and power grab during the detailed survey, and the same laboratory analysis were conducted for these rocks but the results of them will be discussed in the paragraphs of "Detailed Survey".

<Results of Thin Section Observation>

Observation of thin section were conducted for the rocks collected from 93SRGC01, 93SRGC11 and 93SRGC18. Microphotographs are shown in Fig. 4-2-2-1. The results are described hereunder;

· 93SRGC01 .... "Olivine Basalt"

This sample was acquired from beneath the 350cm thick sediments of 93SRGC01 as a rock fragment with a diameter of 6 cm. Macroscopically, it is a massive, vesicular rock assuming dark gray ~ black. It was conspicuous gas cavities caused by vesiculation. Whitened phenocryst of plagioclase is identified, which shows porphyritic appearance.

Microscopically, it is a basalt scattering with phenocrysts of olivine and plagioclase. These phenocrysts often form congregated shapes. Conspicuous gas cavities (maximum diameter: about 0.5 mm) caused by vesiculation are recognized in its groundmass and presenting a chilled texture but it is not a vitreous texture. Hardly altered.

The plagioclase of the phenocrysts is euhedral ~ subhedral with a maximum diameter of about 1.5 mm. A small amount of which is identified. It sometimes contains glass inclusions. Phenocrysts of plagioclase and olivine often form their cumulophyritic texture. The olivine of the phenocrysts is euhedral ~ subhedral with a maximum diameter of about 1.0 mm. A very small amount ~ small amount of which is identified. It sometimes contains glass inclusions. Plagioclase in groundmass presents a long piller shape. Fine ~ needle-shaped olivine crystal

93SRGC11-01 Reflecting

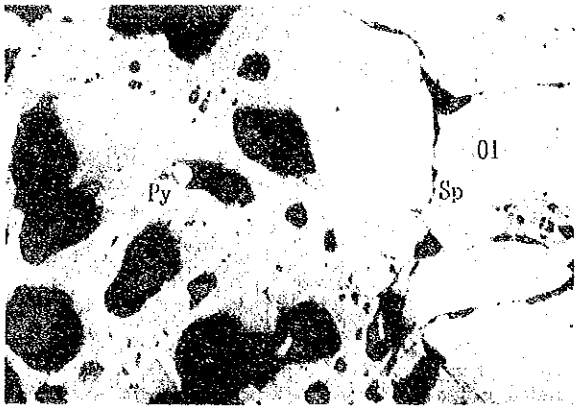


93SRGC11-01 Reflecting

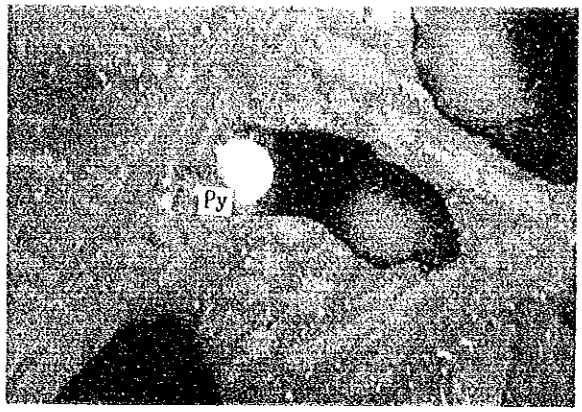


93SRGC11-01 Open nicol

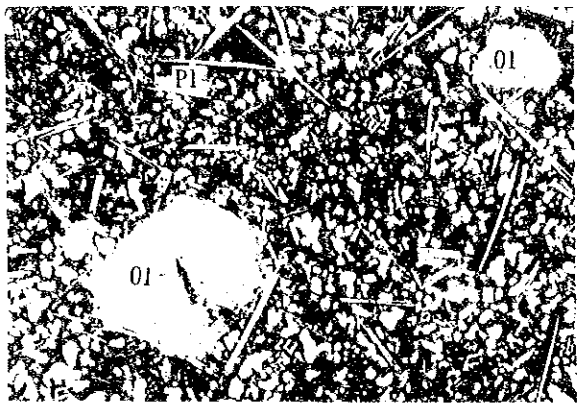


93SRGC11-01 Cross nicol


Abbreviation

| | | | |
|---|---|---|---|
| Py : Pyrite | Sp : Sphalerite | Ol : Olivine |
| Pl : Plagioclase | Opx : Ortho pyroxene | Cpx : Chino pyroxene |
| Vg : Ogns cavity | | |

Figure 4-2-2-1 Microscopic Photos of Rocks on Regional Survey (1)

93SRGC18-05 Open nicol

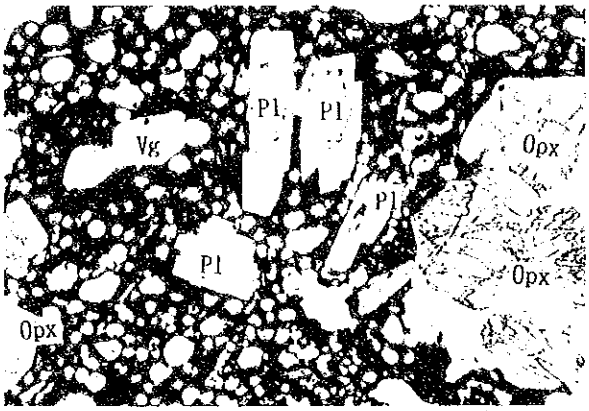


93SRGC18-05 Cross nicol

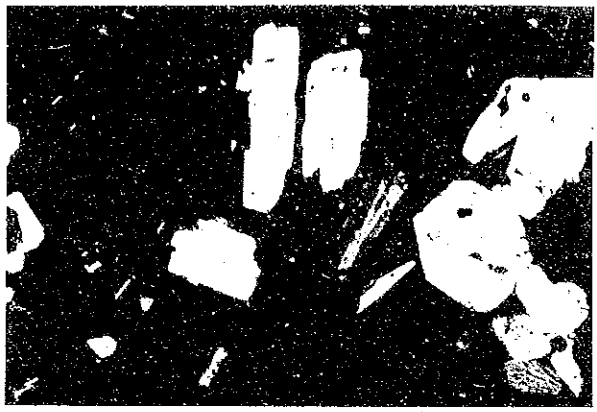


93SRGC01-09 Open nicol

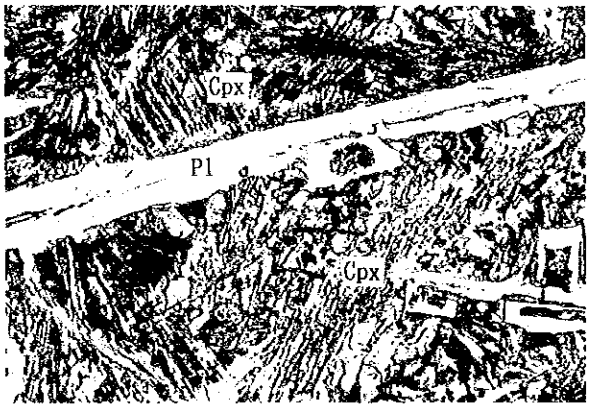


93SRGC01-09 Cross nicol


Abbreviation

| | | |
|---|---|---|
| Py : Pyrite | Sp : Sphalerite | Ol : Olivine |
| Pl : Plagioclase | Opx : Ortho pyroxene | Cpx : Chino pyroxene |
| Vg : Ogns cavity | | |

Figure 4-2-2-1 Microscopic Photos of Rocks on Regional Survey (2)

(maximum diameter: about 0.5 mm) presents a comblike ~ twig-shaped texture grown from the surface of a long piller-shaped plagioclase and comblike ~ twing-shaped clinopyroxene crystal (maximum diameter: about 0.4 mm) are characteristically observed.

The phenocrystic mineral assemblage of plagioclase and olivine identified in this sample is a characteristic of typical ridge basalt. Furthermore, comblike ~ twing-shaped fine olivine, clinopyroxene and needle-shaped olivine grown around a long piller-shaped plagioclase in the groundmass are considered to be textures characteristic of ridge basalt resulted from rapidly grown olivine in the groundmass chilled after the submarine eruption. From the point that clinopyroxenes are found in the groundmass, the differentiation of this sample may have advanced a little bit more than that of 93SRGC11 which will be discussed later.

· 93SRGC11 .... "Olivine Basalt"

Sediments were not collected from 93SRGC11 and this sample was acquired directly from the seafloor in a form of rock fragment with a diameter of less than 5 cm. Macroscopically, it is a massive, slightly vesicular rock assuming dark gray ~ black. There are a small quantity of gas cavities caused by vesiculation.

Microscopically, it is a basalt scattering with olivine phenocrysts. Its plagioclase presents a long-piller-shaped (about 0.5 mm long) and occurs as microphenocryst ~ groundmass. Gas cavities (maximum diameter: about 0.5 mm) caused by vesiculation are identified in the groundmass and presenting a chilled texture but it is not a vitreous texture. Hardly altered.

The plagioclase of the phenocrysts is euhedral with a maximum diameter of about 0.5 mm. Only a small amount of which is identified as long piller-shaped microphenocryst. The olivine of the phenocryst is euhedral ~ subhedral with a maximum diameter of about 1.2 mm. A very small amount ~ small amount of which is identified in the form of cumulophyritic texture.

Most of the plagioclases of the groundmass present a long piller shape (maximum diameter: about 0.5 mm). Very fine olivine presenting a comblike ~ twig-shaped texture grown from the surface of the long piller-shaped plagioclase is characteristically observed.

As we identified macroscopically sulfide minerals, we conducted the microscopy under a reflecting microscope. As a result, a trace of pyrite > galena >

tetrahedrite and euhedral ~ subhedral spinel (maximum diameter: about 0.05 mm) included in olivine phenocryst are identified. Pyrite (maximum diameter: about 0.03 mm) occurs in gas cavities by presenting an euhedral ~ anhedral colloform ~ concentric. Both galena (maximum diameter: about 0.01 mm) and tetrahedrite (maximum diameter: about 0.03 mm) are presenting an indefinite form and exist paragenetically in the gas cavities.

Basaltic texture in which the crystallization of plagioclase phenocryst advances slower than that of olivine phenocryst is considered the evidence of either low degree of partial melting or genesis of magma in deep crust. Which has a tendency to erupt at an area slightly away from a ridge spreading center. A ridge spreading center is estimated to be in around the sampling point of this sample from the submarine topography which is inconsistent with the above hypothesis. Comblike ~ twig-shaped fine olivine grown around long piller-shaped plagioclase in the groundmass is considered to be textures characteristic of ridge basalt resulting from rapidly grown olivine in the groundmass chilled after the submarine eruption.

Furthermore, from the reason that galena was found in this sample, we can presume that there exists (1) a granitic continental crust or (2) an island arc environment in which the granitic continental crust is being built, or (3) a differentiated dacite ~ rhyolitic magma in this area's bed rock.

· 93SRGC18 .... "Two-Pyroxene Basaltic Andesite"

This sample was acquired from beneath the 25 cm thick sediments of 93SRGC18 in a form of granular rock fragments with diameter of less than 1 cm. Macroscopically, it is a rock with conspicuous plagioclase phenocrysts assuming dark gray ~ black.

Microscopically, it is a basaltic andesite scattering with clinopyroxene · orthopyroxene · plagioclase phenocrysts and often forming cumulophyritic texture. Gas cavities (maximum diameter: about 0.5 mm) caused by vesiculation are recognized in its groundmass. The groundmass is vitreous ~ microcrystalline. Hardly altered.

The plagioclase of the phenocryst is euhedral ~ subhedral with maximum diameter of 1.5 mm. A small amount of which was identified. Glass inclusions are occasionally included in it. The clinopyroxene and orthopyroxene of phenocryst are euhedral ~ subhedral with a maximum diameter of about 2.0 mm. A trace ~ small quantity of them are identified. They often form cumulophyritic texture.

A trace of plagioclase presenting a long piller shape (maximum diameter: about 0.5 mm) is identified in the groundmass.

Well-vesiculate groundmass is considered as showing high content of volatile components in magma. Also it is expected to have the chemical composition of andesite. From above, this sample is presumed to be a product of activities under an island arc environment (e.g. back arc basin) rather than a ridge basalt.

<Whole Rock Analysis>

Whole rock analysis was conducted on the rock sample acquired at 93SRGC11.

This sample is identical with the sample identified as "olivine basalt" by the observation of thin sections. The analytical methods are as follows:

ICP emission analysis for : $Al_2O_3$, $TiO_2$, BaO, MgO, CaO, MnO, $P_2O_5$, Total-Fe

Atomic absorption analysis for: $Na_2O$, $K_2O$

Titration method for : FeO

Gravimetric method for : $SiO_2$, LOI (1000℃)

As for $Fe_2O_3$, we calculated it by deducting FeO from Total-Fe, 0.01% of detection limit was applied to each case. The results are shown in Table 4-2-2-1. The results of norm calculation and the result of "differentiation index" calculation are also shown in the same Table.

## 4-3 Results of Survey

Chemical analysis and powder X-ray diffraction test were conducted on 139 samples of seafloor sediments collected from this area. A list of analytic samples is shown in Appendix Table 3.

### 1) Chemical Analysis

The analytical components and limits of detection are as follows: $SiO_2$, $TiO_2$, $Al_2O_3$, $Fe_2O_3$, FeO, MnO, MgO, CaO, BaO, $Na_2O$, $K_2O$, $P_2O_5$ and LOI (the lower detection limit of the above 13 components is 0.01% and the lower limits of detection for the following 25 elements are shown in the parentheses respectively), Ag (0.02ppm), Cu (0.2ppm), Pb (0.5ppm), Zn (1ppm), Mn (5ppm), Total-S (0.001%), Cd (0.1ppm), Ni (1ppm), Co (1ppm), As (0.2ppm), Sb (0.2ppm), Hg (10ppb), Ba (5ppm), Sr (1ppm), Cl (100ppm), P (0.005%), $SO_4$ (0.01%), $CO_2$ (0.1%), Cr (2ppm), V (1ppm), Tl (0.1ppm), B (5ppm), Li (1ppm), Rb

Table 4-2-2-1 Result of whole rock analysis (93SRGC11)

| | | | |
|---|---|---|---|
| Chemical Composition | Major Element Contents (%) | $SiO_2$ | 51.03 |
| | | $TiO_2$ | 0.82 |
| | | $Al_2O_3$ | 15.56 |
| | | $Fe_2O_3$ | 2.99 |
| | | FeO | 4.70 |
| | | MnO | 0.14 |
| | | MgO | 9.86 |
| | | CaO | 10.31 |
| | | $Na_2O$ | 2.35 |
| | | $K_2O$ | 0.39 |
| | | $P_2O_5$ | 0.09 |
| | | BaO | <0.01 |
| | | LOI | 0.78 |
| | | Total | 99.02 |
| Norm calculation | Normative mineral composition | Q | 1.33 |
| | | C | 0.00 |
| | | OR | 2.31 |
| | | AB | 19.87 |
| | | AN | 30.76 |
| | | NE | 0.00 |
| | | AC | 0.00 |
| | | KS | 0.00 |
| | | WO | 0.00 |
| | | DI-WO | 8.26 |
| | | DI-EN | 6.17 |
| | | DI-FS | 1.27 |
| | | HY-EN | 18.37 |
| | | HY-FS | 3.79 |
| | | OL-FO | 0.00 |
| | | OL-FA | 0.00 |
| | | MT | 4.33 |
| | | HM | 0.00 |
| | | IL | 1.56 |
| | | TN | 0.00 |
| | | PF | 0.00 |
| | | AP | 0.21 |
| | | TOTAL | 98.23 |
| | Differentiation index | | 23.51 |

(5ppm) and U (0.2ppm).

The methods of analysis are as follows: ICP emission analysis for: $SiO_2$, $TiO_2$, $Al_2O_3$, $Fe_2O_3$, MnO, MgO, CaO, $Na_2O$, $K_2O$ and $P_2O_5$. Neutrolization titration method for: FeO. Ignition loss at 1000℃ for: LOI, $SO_4$ was measured by the gravimetric method. $CO_2$ was measured by LECO. ICP emission analysis after the decomposition and extraction by hydrochloric acid - potassium chlorate or hydrofluoric acid - nitric acid - perchloric acid for: Ag, Cu, Pb, Zn, Mn, Cd, Ni, Co, As, Sb, Ba, Sr, P, Cr and V. After the decomposition by perchloric acid - nitric acid and hydrochloric acid - hydrofluoric acid for Hg, Tl, S, Rb, Li, Cl, B and U, cold vapour of Hg and Tl were measured by the atomic absorption method. S was measured by a high frequency induction heating infrared absorption photometer (LECO). Rb and Li were determined by the atomic absorption method. B, Cl and U were determined by the neutron activation analysis (NAA). BaO was calculated from Ba.

The results are shown in Appendix Table 4.

2) X-ray Diffraction

With the object of clarifying the mineral composition and quantitative ratio of the samples of muddy substances, powder X-ray diffraction was conducted on them by the random orientation method and preferred orientation method. The random orientation method was conducted on 139 samples identical with the samples that underwent the chemical analysis and the preferred orientation method was conducted on 37 samples identical with the samples that underwent the discrimination of foraminiferous fossils and the mechanical analysis. The 37 samples that underwent the preferred orientation method are in common with a part of the 139 samples that underwent the random orientation method.

The samples for the random orientation method dried naturally, crushed and measured. The conditions of X-ray diffraction are as follows:

Equipment used : diffractometer Geigerflex RAD C (Rigaku)
Bulb Normal Focus, Cu anode
Slit system 1° - 0.3 mm - 1°
Voltage/current 30KV/15mA

Condition of diffraction: Scan angle 2 ～ 70°
Scanning speed 4° /min.

The samples for the preferred orientation method dried naturally, crushed and were

conducted by the sedimentation method several times, and then suspended matters acquired were undergone the X-ray diffraction by the random orientation method as well as by the preferred orientation method. If necessary, the test pieces underwent chemical treatments such as ethylene glycol treatment, hydrochloric acid treatment and heat treatment before conducting the X-ray diffraction. The conditions of X-ray diffraction are as follows:

Equipment used : identical with the above-mentioned equipment
Conditions of diffraction: Scan angle 2 ~ 4° (samples for random and preferred orientation), 2 ~ 20° (samples for preferred orientation and chemical treatment)
Scanning speed 4° /min. (samples for random and preferred orientation)
2° /min. (samples for preferred orientation and chemical treatment)

The results of the random orientation method on the 139 samples are shown in Table 4-3-2-1 and the results of the preferred orientation method on the 37 samples are shown in Table 4-3-2-2.

Calcite, plagioclase (close to anorthite), halite, quartz and pyroxene (augite) are identified in most of the 139 samples undergone the random orientation method, and tridymite and amphibole (hornblende) are identified in half of them. Quantitatively, the former are abundant in the samples of 93SR (the rest is omitted) GC02, GC03, GC05, LC06, LC07 and GC19 cores. The latter are abundant in the samples of GC02, GC03, GC04, GC05, LC06, GC13, GC19 and GC24 cores. As for clay minerals, chlorite is commonly detected, though the diffraction intensity is very weak, from the samples with the exception of GC08, GC09, GC10, GC12, GC16, GC18 and GC19 cores. A trace of montmorillonite (samples GC03-04, LC06-14, GC23-06, GC24-04 and GC24-06) and muscovite (samples GC05-03 and LC06-04) are identified. Besides, olivine (samples GC16-04, GC18-01, GC18-02 and LC20-04), magnetite (samples GC01-07, GC01-08, GC04-03, GC05-06, LC06-14, GC09-05, GC18-04, GC19-02, GC19-04, LC20-05 ~ 09, GC26-01 and GC26-04), pyrite (sample GC01-01, GC03-02, GC03-03, GC04-02, LC06-08, LC06-10, LC06-11, LC06-13, LC07-03 and GC09-03) and sphalerite (samples GC26-02 and GC26-03) occur,

Table 4-3-2-1 Results of X-ray diffraction method of whole sediments (1)

| Sample No. | Quartz | Tridymite | Plagioclase | Olivine | Pyroxene | Amphibole | Calcite | Halite | Montmori-llonite | Chlorite | Mica | Pyrite | Sphalerite | Magnetite |
|---|---|---|---|---|---|---|---|---|---|---|---|---|---|---|
| 93SRGC 01-01 | + | ± | + | | ± | | ++ | + | | | | - | | |
| 93SRGC 01-02 | + | | + | | ± | | ++ | + | | ± | | | | - |
| 93SRGC 01-03 | + | | + | | ± | | ++ | + | | - | | | | |
| 93SRGC 01-04 | + | | + | | ± | | ++ | + | | ± | | | | |
| 93SRGC 01-05 | + | ± | + | | ± | | ++ | + | | ± | | | | |
| 93SRGC 01-06 | + | ± | + | | ± | | ++ | + | | ± | | | | |
| 93SRGC 01-07 | + | | + | | ± | | ++ | + | | ± | | | | |
| 93SRGC 01-08 | + | - | + | | + | - | ++ | + | | - | | | | |
| 93SRGC 02-01 | + | ± | + | | ± | | ++ | + | | ± | | | | |
| 93SRGC 02-02 | + | ± | + | | ± | | ++ | + | | | | | | |
| 93SRGC 02-03 | + | ± | + | | ± | | ++ | + | | | | | | |
| 93SRGC 02-04 | + | ± | + | | ± | ± | ++ | + | | ± | | | | |
| 93SRGC 02-05 | + | | + | | ± | | ++ | + | | | | | | |
| 93SRGC 02-06 | + | ± | + | | ± | | ++ | + | | ± | | | | |
| 93SRGC 02-07 | + | ± | + | | ± | + | ++ | + | | - | | | | |
| 93SRGC 02-08 | + | ± | + | | - | - | ++ | + | | | | | | |
| 93SRGC 03-01 | + | ± | + | | ± | ± | ++ | + | | ± | | ± | | |
| 93SRGC 03-02 | + | ± | + | | ± | ± | ++ | + | | ± | | ± | | |
| 93SRGC 03-03 | + | ± | + | | ± | ± | ++ | + | | ± | | | | |
| 93SRGC 03-04 | + | ± | + | | ± | ± | ++ | + | | ± | | | | |
| 93SRGC 03-05 | + | ± | + | | ± | ± | ++ | + | ± | ± | | | | |
| 93SRGC 03-06 | + | ± | + | | ± | ± | ++ | + | | ± | | | | |
| 93SRGC 04-01 | + | | + | | ± | ± | ++ | + | | ± | | ± | | |
| 93SRGC 04-02 | + | | + | | ± | | ++ | + | | ± | | | | ± |
| 93SRGC 04-03 | + | ± | + | | ± | ± | ++ | + | | ± | | | | |
| 93SRGC 04-04 | + | | + | | ± | | ++ | + | | ± | | | | |
| 93SRGC 04-05 | + | | + | | ± | | ++ | + | | ± | | | | |
| 93SRGC 04-06 | + | ± | + | | ± | ± | ++ | + | | ± | | | | |
| 93SRGC 04-07 | + | ± | + | | ± | ± | ++ | + | | ± | | | | |
| 93SRGC 05-01 | + | | + | | ± | | ++ | + | | ± | | | | |
| 93SRGC 05-02 | ± | ± | + | | + | | ++ | + | | + | | | | |
| 93SRGC 05-03 | + | ± | + | | + | | ++ | + | | + | ± | | | |
| 93SRGC 05-04 | + | ± | + | | + | | ++ | + | | | | | | |
| 93SRGC 05-05 | + | ± | + | | + | + | ++ | + | | | | | | |
| 93SRGC 05-06 | + | ± | + | | + | ± | ++ | + | | ± | | | | ± |
| 93SRGC 05-07 | + | ± | + | | ± | ± | ++ | + | | ± | | | | |
| 93SRLC 06-01 | + | | + | | ± | | ++ | + | | ± | | | | |
| 93SRLC 06-02 | + | | + | | ± | + | ++ | + | | ± | | | | |
| 93SRLC 06-03 | + | ± | + | | | ± | ++ | + | | ± | ± | | | |
| 93SRLC 06-04 | + | | + | | ± | ± | ++ | + | | ± | | | | |
| 93SRLC 06-05 | + | | ++ | | ± | ± | ++ | + | | | | | | |
| 93SRLC 06-06 | + | | + | | ± | ± | ++ | + | | | | | | |
| 93SRLC 06-07 | + | | + | | ± | ± | ++ | + | | | | | | |
| 93SRLC 06-08 | + | ± | ++ | | ± | + | ++ | + | | | | ± | | |
| 93SRLC 06-09 | + | | + | | ± | + | ++ | + | | | | | | |
| 93SRLC 06-10 | + | ± | ++ | | ± | ± | ++ | + | | | | ± | | |
| 93SRLC 06-11 | + | ± | ++ | | ± | ± | ++ | + | | | | | | |
| 93SRLC 06-12 | + | ± | + | | ± | | ++ | + | | | | ± | | |
| 93SRLC 06-13 | + | | ++ | | ± | | ++ | + | | ± | | | | |
| 93SRLC 06-14 | + | | + | | ± | | ++ | + | ± | ± | | | | ± |
| 93SRLC 06-15 | + | ± | + | | ± | ± | ++ | + | | ± | | | | |
| 93SRLC 07-01 | + | ± | + | | + | | ++ | + | | | | | | |
| 93SRLC 07-02 | + | ± | ++ | | + | | ++ | + | | ++ | | ± | | |
| 93SRLC 07-03 | + | ± | ++ | | + | | ++ | ± | | | | | | |
| 93SRLC 07-04 | + | ± | + | | + | | ++ | ± | | | | | | |
| 93SRLC 07-05 | + | ± | + | | + | | ++ | ± | | | | | | |
| 93SRLC 07-06 | + | ± | + | | ± | | ++ | ± | | | | | | |
| 93SRLC 07-07 | + | ± | + | | ± | ± | ++ | - | | | | | | |
| 93SRLC 07-08 | + | | + | | ± | | ++ | + | | | | | | |
| 93SRLC 07-09 | + | | + | | + | | ++ | ± | | | | | | |
| 93SRGC 08-01 | + | | + | | | | ++ | + | | | | | | |
| 93SRGC 08-02 | ± | | + | | | | ++ | + | | | | | | |
| 93SRGC 08-03 | + | | + | | | | ++ | + | | | | | | |
| 93SRGC 08-04 | + | | + | | ± | | ++ | + | | | | | | |
| 93SRGC 08-05 | + | | + | | ± | | ++ | + | | | | | | |
| 93SRGC 08-06 | + | | + | | ± | | ++ | + | | | | | | |
| 93SRGC 09-01 | ± | | + | | + | | ++ | + | | | | ± | | |
| 93SRGC 09-02 | + | | + | | + | | ++ | + | | | | | | |
| 93SRGC 09-03 | ± | | + | | + | | ++ | + | | | | ± | | |
| 93SRGC 09-04 | ± | | ++ | | + | | ++ | + | | | | | | |
| 93SRGC 09-05 | ± | | ++ | | + | | ++ | + | | | | | | ± |

Note : Low crystalline silica (cristobalite ~ opal) seems to exist in 93SRLC07-03~05 samples.

Legend : ++ ; large peak, + ; small peak, ± ; little or uncertain peak.

Table 4-3-2-1 Results of X-ray diffraction method of whole sediments (2)

| Sample No. | Quartz | Tridymite | Plagioclase | Olivine | Pyroxene | Amphibole | Calcite | Halite | Montmori-llonite | Chlorite | Mica | Pyrite | Sphalerite | Magnetite |
|---|---|---|---|---|---|---|---|---|---|---|---|---|---|---|
| 93SRGC 10-01 | ± | | +++ | | ± | | ++ | +++ | | | | | | |
| 93SRGC 10-02 | | | +++ | | ± | | ++ | +++ | | | | | | |
| 93SRGC 10-03 | | | +++ | | ± | | ++ | +++ | | | | | | |
| 93SRGC 10-04 | ± | | +++ | | ± | | ++ | +++ | | | | | | |
| 93SRGC 10-05 | ± | | +++ | | ± | | ++ | +++ | | | | | | |
| 93SRGC 10-06 | ± | | +++ | | ± | ± | ++ | +++ | | | | | | |
| 93SRGC 12-01 | ± | | + | | + | | ++ | +++ | | | | | | |
| 93SRGC 12-02 | + | | +++ | | ++ | | ++ | +++ | | | | | | |
| 93SRGC 12-03 | + | ± | +++ | | ++ | | ++ | +++ | | | | | | |
| 93SRGC 12-04 | + | | +++ | | ++ | | ++ | +++ | | | | | | |
| 93SRGC 12-05 | + | | +++ | | ++ | + | ++ | +++ | | | | | | |
| 93SRGC 13-01 | + | | + | | ± | | ++ | +++ | | + | | | | |
| 93SRGC 13-02 | ++ | | +++ | | ± | ± | ++ | +++ | | ± | | | | |
| 93SRGC 13-03 | ++ | | +++ | | ± | ± | ++ | +++ | | ± | | | | |
| 93SRGC 13-04 | + | | +++ | | ± | | ++ | +++ | | ± | | | | |
| 93SRGC 13-05 | ++ | | +++ | | ± | ± | ++ | +++ | | ± | | | | |
| 93SRGC 13-06 | ++ | | +++ | | ± | | ++ | +++ | | ± | | | | |
| 93SRGC 13-07 | ++ | | +++ | | ± | | ++ | +++ | | ± | | | | |
| 93SRGC 13-08 | ++ | | +++ | | ± | + | + | ++ | | ± | | | | |
| 93SRLC 14-01 | + | | + | | + | | ++ | ++ | | + | | | | |
| 93SRLC 14-02 | ++ | | ++ | | - | | ++ | ++ | | ± | | | | |
| 93SRLC 14-03 | ++ | | ++ | | ± | | ++ | ++ | | | | | | |
| 93SRGC 15-01 | + | | + | | + | | ++ | + | | ± | | | | |
| 93SRGC 15-02 | ± | | + | | + | | ++ | ++ | | ± | | | | |
| 93SRGC 15-03 | + | | + | | + | | ++ | ++ | | ± | | | | |
| 93SRGC 15-04 | + | | + | | ± | - | ++ | ++ | | ± | | | | |
| 93SRGC 15-05 | + | | + | | - | ± | ++ | ++ | | ± | | | | |
| 93SRGC 15-06 | + | | + | | ± | ± | ++ | ++ | | ± | | | | |
| 93SRGC 16-01 | + | | + | | ± | | ++ | + | | | | | | |
| 93SRGC 16-02 | + | | + | | ± | | ++ | + | | | | | | |
| 93SRGC 16-03 | + | | + | | ± | | ++ | + | | | | | | |
| 93SRGC 16-04 | + | | + | ± | ± | | ++ | + | | | | | | |
| 93SRGC 16-05 | + | | + | | ± | | ++ | + | | | | | | |
| 93SRGC 18-01 | + | | + | ± | + | | + | + | | | | | | |
| 93SRGC 18-02 | + | | ++ | ± | + | | + | + | | | | | | |
| 93SRGC 18-03 | + | | + | | + | | ++ | ± | | | | | | ± |
| 93SRGC 18-04 | + | | ++ | | + | | + | + | | | | | | |
| 93SRGC 19-01 | + | | ++ | | ± | ± | + | + | | | | | | |
| 93SRGC 19-02 | + | ± | ++ | | + | ± | ++ | + | | | | | | + |
| 93SRGC 19-03 | + | ± | ++ | | + | | ++ | + | | | | | | ± |
| 93SRGC 19-04 | | ± | + | | | + | + | + | | | | | | |
| 93SRLC 20-01 | + | | + | | + | | ++ | + | | | | | | |
| 93SRLC 20-02 | + | | + | | + | | ++ | + | | | | | | |
| 93SRLC 20-03 | ± | | + | | + | | ++ | + | | ± | | | | ± |
| 93SRLC 20-04 | ± | ± | ++ | + | + | | ++ | + | | ± | | | | ± |
| 93SRLC 20-05 | + | | + | | + | | ++ | ± | | ± | | | | ± |
| 93SRLC 20-06 | | | ++ | | + | | + | + | | ± | | | | ± |
| 93SRLC 20-07 | | | ++ | | + | | ++ | ± | | + | | | | ± |
| 93SRLC 20-08 | + | | - | | + | | + | + | | | | | | |
| 93SRLC 20-09 | + | | + | | + | | ++ | + | | | | | | |
| 93SRLC 20-10 | ± | | ++ | | + | | + | ++ | | | | | | |
| 93SRGC 23-01 | + | | + | | + | | ++ | + | | ± | | | | |
| 93SRGC 23-02 | + | ± | ++ | | + | | + | + | | ± | | | | |
| 93SRGC 23-03 | + | | + | | + | | ++ | + | | ± | | | | |
| 93SRGC 23-04 | + | | + | | + | | + | + | | ± | | | | |
| 93SRGC 23-05 | + | | + | | ± | | ++ | + | | ± | | | | |
| 93SRGC 23-06 | | ± | ++ | | + | | + | + | + | ± | | | | |
| 93SRGC 24-01 | + | | + | | ± | ± | ++ | + | | ± | | | | |
| 93SRGC 24-02 | + | | + | | + | ± | ++ | + | | ± | | | | |
| 93SRGC 24-03 | + | | + | | + | ± | ++ | + | | ± | | | | |
| 93SRGC 24-04 | + | | + | | + | ± | ++ | + | | ± | | | | |
| 93SRGC 24-05 | + | | + | | + | ± | ++ | + | ± | ± | | | | |
| 93SRGC 24-06 | + | | + | | + | + | + | + | + | + | | | | |
| 93SRGC 26-01 | ± | | ++ | | + | | + | + | | ± | | | ± | ± |
| 93SRGC 26-02 | + | | ++ | | + | | ++ | + | | | | | | |
| 93SRGC 26-03 | + | | ++ | | + | | + | + | | | | | | |
| 93SRGC 26-04 | + | | + | | + | | ++ | + | | ± | | | ± | ± |
| 93SRGC 26-05 | + | | ++ | | + | ± | ++ | ± | | ± | | | | |

Note : Low crystalline silica (cristobalite ~ opal) seems to exist in 93SRGC19-04 samples.

Legend : ++ ; large peak, + ; small prak, ± ; little or uncertain peak.

Table 4-3-2-2 Results of X-ray diffraction method of clay minerals in sediments

| Sample No. | Clinochlore | Ferroan montmorillonite |
|---|---|---|
| 93SRLC 06-01 | + | |
| 93SRLC 06-02 | ± | + |
| 93SRLC 06-03 | + | + |
| 93SRLC 06-04 | + | + |
| 93SRLC 06-05 | + | |
| 93SRLC 06-06 | | |
| 93SRLC 06-07 | + | + |
| 93SRLC 06-08 | ± | |
| 93SRLC 06-09 | + | |
| 93SRLC 06-10 | ± | + |
| 93SRLC 06-11 | ± | |
| 93SRLC 06-12 | ± | ± |
| 93SRLC 06-13 | + | ± |
| 93SRLC 06-14 | + | + |
| 93SRLC 06-15 | + | + |
| 93SRLC 07-01 | ± | + |
| 93SRLC 07-02 | ± | + |
| 93SRLC 07-03 | + | + |
| 93SRLC 07-04 | ± | + |
| 93SRLC 07-05 | ± | + |
| 93SRLC 07-06 | ± | ± |
| 93SRLC 07-07 | ± | ± |
| 93SRLC 07-08 | ± | ± |
| 93SRLC 07-09 | ± | ± |
| 93SRLC 14-01 | ± | ± |
| 93SRLC 14-02 | ± | ± |
| 93SRLC 14-03 | ± | + |
| 93SRLC 20-01 | + | + |
| 93SRLC 20-02 | | + |
| 93SRLC 20-03 | ± | + |
| 93SRLC 20-04 | ± | + |
| 93SRLC 20-05 | + | + |
| 93SRLC 20-06 | ± | + |
| 93SRLC 20-07 | + | + |
| 93SRLC 20-08 | + | + |
| 93SRLC 20-09 | + | + |
| 93SRLC 20-10 | ± | + |

Note : Kinds of mineral and intensity of diffraction peak were decided by random orientation method

Legend : + ; small peak, ± ; little or uncertain peak.

but we cannot accurately determine them because the diffraction lines of these minerals are often masked by other minerals. Furthermore, diffraction lines presumed to be serpentine and orthoclase are recognized in some samples but we did not list them because we cannot accurately distinguish them from chlorite and plagioclase. Also, we recognized wide swollen backgrounds at 3 ～ 4Å in some samples (LC07-03 ～ 05 and GC19-04) from which we can presume the existence of low crystalline silica (cristobalite～ opal). But we did not list them due to uncertainty.

In the aggregate, the difference of mineral spieces among the samples is small, though there are some differences of diffraction intensity. We may safely say that the 139 samples roughly show the identical mineral compositions.

All of the 37 samples for the preferred orientation have very few clay minerals. For this reason, we had conducted sedimentation method several times but we could get only an extremely small amount of suspended matters. In order to get 1 or 2 grams of suspended matters, we needed average 200 g to 400 g of original samples. Nevertheless, there are only few diffraction lines of clay minerals and diffraction lines of other minerals such as strong calcite, obvious plagioclase, very small or obscure quartz, pyroxene and tridymite got mixed with them. Also, amphibole got mixed with some samples. Such mineral compositions are all identical to the 139 samples that had undergone the random orientation method. In order to check these mixed substances, we did the preferred orientation test twice but the results of diffraction were the same.

The species of clay mineral in the 37 samples is identified as clinochlore and montmorillonite rich in iron. Which is identical to all the 37 samples. The diffraction intensity of each sample is very small. So, we could not clarify its polytype and the detailed composition of clay mineral.

This clinochlore has very weak diffraction lines at 14Å and 7Å. It also has diffraction lines at 3.5Å and 2.5Å. The samples of LC06 core and LC14 core have the diffraction intensity of 14Å≧7Å, the samples of LC07 core and LC20 core have 14Å >7Å. The peak of (003) is not detected. And the diffraction lines disappeared completely when it was treated by hydrochloric acid. So we can presume it as clinochlore with Mg and Fe but poor Al.

This montmorillonite has weak but obvious diffraction line at 15Å. But it does not have other obvious peaks, especially, a diffraction line at 5Å, so we can identify it with montmorillonite rich in Fe (it also has a possibility of being saponite). The sample of LC20 core has double peaks reaching 13 ～ 17Å which